JONATHAN DALLAIRE

THERMAL CONDUCTIVITY OF CARBON NANOTUBES FROM EQUILIBRIUM MOLECULAR DYNAMICS SIMULATIONS: SENSITIVITY TO MODELING AND SIMULATION PARAMETERS

Mémoire présenté
à la Faculté des études supérieures et postdoctorales de l'Université Laval
dans le cadre du programme de maîtrise en génie mécanique
pour l'obtention du grade de maître ès sciences (M. Sc.)

DÉPARTEMENT DE GÉNIE MÉCANIQUE
FACULTÉ DES SCIENCES ET DE GÉNIE
UNIVERSITÉ LAVAL
QUÉBEC

2012

CONTENTS

FIGURE CAPTIONS

RÉSUMÉ

Le présent travail vise à apporter certaines pistes de solution concernant certaines controverses sur l'estimation de la conductivité thermique des nanotubes de carbone par simulation de dynamique moléculaire à l'équilibre avec conditions aux limites périodiques et la formule de Green-Kubo. Entre autre, différents auteurs obtiennent des résultats pouvant parfois varier de plusieurs ordres de grandeur pour un même type de nanotube. Il n'y a toutefois que très peu d'études jusqu'à ce jour tentant d'expliquer ces contradictions. Dans la première partie du projet, on détermine les paramètres numériques pouvant influencer la conductivité thermique calculée avec une méthode de dynamique moléculaire à l'équilibre. On effectue ensuite une analyse de sensibilité pour plusieurs de ces paramètres afin de déterminer de quelle manière ils influencent la conductivité thermique calculée (chapitres 3 et 4). Finalement, on présente une étude sur le phénomène de fréquence de coupure lors du calcul de la conductivité thermique (chapitre 5).

ABSTRACT

The goal of the present work is to give possible explanations for some of the discrepancies found in literature concerning the estimation of the thermal conductivity of carbon nanotubes from equilibrium molecular dynamics simulations with periodic boundary conditions and the Green-Kubo formula. Some of the results presented by different authors are in disagreement for the same type of carbon nanotube (chirality). Up to now, there are still very few studies aiming at explaining these discrepancies. During the first part of the present work, we determine which modeling and simulation parameters can influence the calculated thermal conductivity from equilibrium molecular dynamics simulations. We then perform a sensitivity analysis for many of these parameters in order to understand how each parameter influences the calculated thermal conductivity (Chapters 3 and 4). Finally, we present a study on the frequency cut-off phenomenon when calculating the thermal conductivity of carbon nanotubes (Chapter 5).

AVANT-PROPOS

Ces travaux sont supportés par le Conseil de recherches en sciences naturelles et en génie du Canada (CRSNG) et par le Fonds de recherche du Québec - Nature et technologies (FQRNT). Toutes les simulations ont été effectuées grâce au supercalculateur Colosse du Clumeq à l'Université Laval.

Toutes les publications présentées dans ce mémoire (Chapitres 3 à 5) ont été rédigées par moi-même en tant que premier auteur pendant mes travaux de maîtrise. J'ai développé et implémenté les modèles et lancé les simulations. J'ai également analysé les résultats et dégagé les conclusions se dégageant de ceux-ci qui m'ont servi à la rédaction des différents articles. Mon directeur de recherche, Louis Gosselin, a également participé à la rédaction en tant que second auteur. Il m'a grandement supporté et a participé à la révision et à la correction des articles. Le premier article présenté au Chapitre 3 a été publié dans les actes de la « 2nd International Conference on Nanotechnology : Fundamentals and Applications, 2011 ». Le second article, présenté au Chapitre 4, a été soumis dans le « Journal of Computational Physics ». Finalement, le dernier article présenté au Chapitre 5 sera soumis dans le journal « Applied Physics Letters » lorsque le précédent article sera accepté.

CHAPTER 1: Definition of the problem

1.1 INTRODUCTION

"There's plenty of room at the bottom." Such was the title of a lecture given by the physicist Richard P. Feynman at an American Physical Society meeting at the California Institute of Technology in 1959 (see http://www.zyvex.com/nanotech/feynman.html for a complete version of his lecture). Feynman mentioned, among many other things, that it would be theoretically possible to write an entire encyclopedia on the head of a pin, or to miniaturize computers so much that wires would be ten to a hundred atoms in diameter and electronic circuits would be of the size of a few micrometers. At that time, the idea of manipulating the matter at an atomic scale seemed quite ambitious. However, there have been many experimental and numerical investigations on nanosciences and nanotechnologies during the last decades, and the reality is now far much closer to Feynman's ideas. Thirty years after his lecture, a Japanese physicist, Sumio Iijima, has published a paper that has generated an increased interest in carbon nanotubes (CNTs), a nanostructure that has remarkable electrical and thermal properties [1]. Some investigations on carbon nanotubes have reported very high thermal conductivity, exceeding even that of diamond [2]. Depending on the experimental technique and on the nanotube characteristics, thermal conductivity measurements reported in literature vary approximately from 300 to 10,000 W/m K [3-7].

The experimental measurement of the thermal conductivity of an isolated CNT can prove to be very difficult [3]. Furthermore, the atomic structure of the studied CNTs, which influences their thermal conductivity, is unknown for the experiments previously mentioned, making it difficult to compare the results based on nanotube chiralities [11]. Because of this, numerical models have been developed to gain a better understanding of the heat transfer process in carbon nanotubes. Molecular dynamics (MD) simulations is a numerical tool that can be used to study the thermal properties of CNTs for a given chirality. The most widely used methods include equilibrium molecular dynamics (EMD) and non-equilibrium molecular dynamics (NEMD). Nevertheless, there is no agreement

in literature on the exact value of the thermal conductivity of carbon nanotubes. Moreover, the trends observed can be very different. For example, the effect of the application of external mechanical strain on a carbon nanotube on its thermal conductivity has already been addressed in the past [8-9], but the reported results are in contradiction. The optimal thermal conductivity reported by [8] for a (10, 10) CNT under axial strain was obtained when the CNT was stretched at 2% of its original length. On the opposite, [9] reported that the maximal thermal conductivity value for a (10, 10) CNT was obtained when the CNT was compressed at 6% of its original length. There have been few investigations on the possible reasons for the discrepancies found in literature concerning the numerical calculation of the thermal conductivity of CNTs using MD simulations [10-11]. The present work studies the possible reasons that have not yet been addressed and that could explain discrepancies in literature for the calculation of the thermal conductivity of CNTs using MD simulations.

1.2 PRESENTATION OF CARBON NANOTUBES

The atomic structure of a carbon nanotube can be seen as a graphene sheet wrapped into a cylinder. Carbon nanotubes can have one or more walls, as shown in Fig. 1.3 (which has been reproduced from [12]). Nanotube A is a single-wall carbon nanotube (SWCNT) and nanotube B is a multi-wall carbon nanotube (MWCNT). As a reference, typical lengths, diameters, and inter-wall spacing are indicated in this figure.

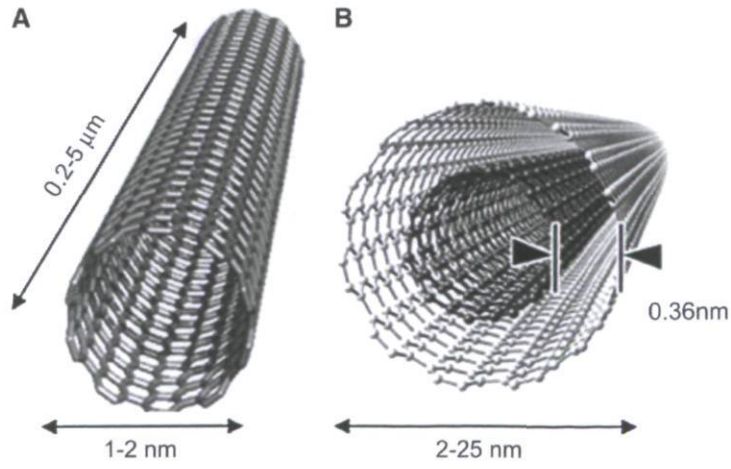

Figure 1.3: Schematic representation of the atomic structure of CNTs, from [12]

The properties of CNTs can vary depending on their chirality. The chirality, or twist, of a carbon nanotube is given by its chiral vector indices (n, m), where n and m are integers of the equation $\vec{C}_h = n\hat{a}_1 + m\hat{a}_2$. The vectors $\hat{a}_1$ and $\hat{a}_2$ are unit vectors in the lattice directions of two-dimensional graphite (see Fig. 1.4) and $\vec{C}_h$ is the chirality vector. Let us consider a nanotube that is cut along the vector $\vec{T}$, a vector tangential to its axis, and then unraveled into a planar sheet. If the line traced by the vector $\vec{T}$ and the line parallel to $\vec{T}$ at the opposite side of the grey box in Fig. 1.4 are superimposed, the original carbon nanotube is obtained. Then, a point on the vector $\vec{T}$ that intersects a carbon atom is taken as the origin of both the tangential and chiral vectors. The armchair line is defined as the one which passes across all the hexagons, separating them in two equal halves, starting from the origin of the vector $\vec{T}$. The second extremity of the chiral vector is given by the point which intersects a carbon atom on the line parallel to $\vec{T}$ at the opposite side of the grey box closest to the armchair line. If the chiral vector is along the armchair line, the nanotube is said to be armchair. If it is along the zigzag line, it is said to be zigzag. In any other case, the nanotube is chiral.

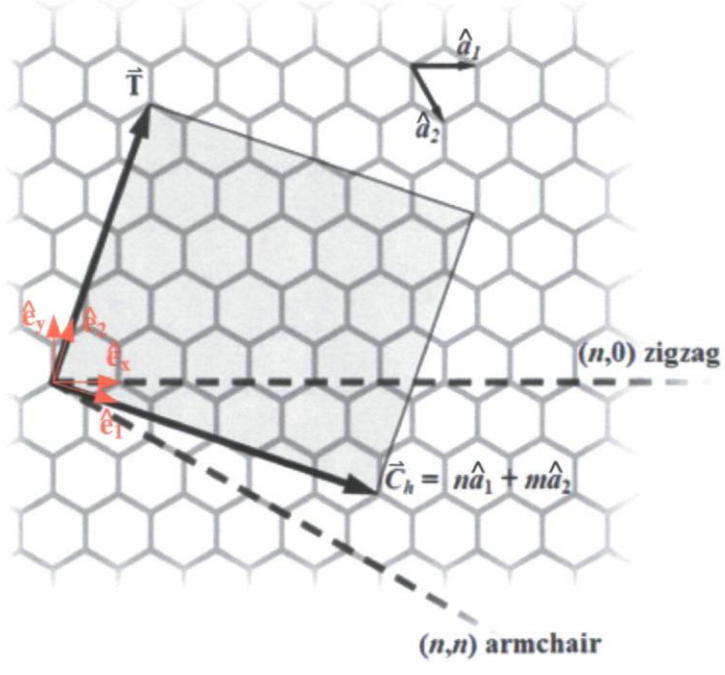

Figure 1.4: Schematic representation of the chiral and tangential vectors

The theoretical diameter d of a SWCNT can be calculated from its (n, m) indices using the following equation [13]:

$$d = \frac{a}{\pi}\sqrt{n^2 + nm + m^2} \tag{1.1}$$

where a = 2.46 Å is the lattice constant of two-dimensional graphite (distance between the two sides of a hexagon), which result in a mean inter-atomic spacing between carbon atoms of $a_{C\text{-}C}$ = 1.421 Å. The chiral angle θ between the chiral vector and the zigzag line can be calculated using Eq. (1.2) [13]. It can take values between $\theta = 0^\circ$ (zigzag nanotube) and $\theta = 30^\circ$ (chiral nanotube).

$$\tan\theta = \frac{\sqrt{3}m}{m+2n} \tag{1.2}$$

1.3 OBJECTIVES

Some possible reasons that could explain discrepancies in literature in terms of the reported thermal conductivity of CNTs have already been addressed. Those reasons mainly consist in modeling or simulation technique parameters of MD simulations. For example, [11] reported that some of the possible reasons for literature discrepancies included length and temperature effects, different choices for the cross-section of CNTs, different choices of inter-atomic potential, different methods (EMD or NEMD), and different boundary conditions. On the other hand, [10] reported that the thermal conductivity values are not significantly influenced by the simulation technique used in NEMD simulations. In other words, the calculated thermal conductivity is not altered when using different integral algorithms or different thermostats during the simulation. Besides modeling and simulation technique, another important part of the calculation of the thermal conductivity using MD simulations resides in the post-treatment of the simulation results. There can be different procedures to follow, depending on the simulation method used.

The main objective of the present dissertation is to study the effect of post-treatment parameters on the calculation of the thermal conductivity of CNTs. This main objective can be separated in three specific objectives, which are: (1) determine which modeling and simulation parameters have an influence on the calculation of the thermal conductivity of carbon nanotubes when using an EMD method, (2) understand how each of those parameters influence the calculation of the thermal conductivity, and (3) determine if the influence of the post-treatment parameters on the calculated thermal conductivity could explain some of the discrepancies found in literature.

1.4 METHODOLOGY

The steps that will be followed in order to achieve those specific objectives will now be explained. First, an extensive review of the literature will help to determine which parameters influence the thermal conductivity, according to the results presented by different authors. Then, a MATLAB routine that can perform MD simulations once interfaced with the LAMMPS software [14] will be implemented. LAMMPS is a free open-source molecular dynamics software from Sandia National Laboratories. The MATLAB routine is required to be able to: (1) calculate the initial position and velocity of each atom of a CNT for a given length and chirality, (2) apply the desired boundary conditions, (3) write in text files the necessary information to run a MD simulation using the LAMMPS software, (4) extract the results from output files generated by LAMMPS, and (5) make the necessary calculations to estimate the thermal conductivity of a carbon nanotube using the simulation results following an EMD simulation. A validation of each step of the simulation will be done to ensure that the EMD procedure is followed properly. A sensitivity analysis will then be performed for the parameters identified in the first step in order to determine how each of them influences the calculated thermal conductivity. Finally, the results and simulation parameters used in other works will be compared with those in the present work in order to determine if using different simulation parameters will result in very different calculated thermal conductivities. Since the time required to run MD simulations can be very long, all simulations are performed on the supercomputer Colosse (part of Clumeq). The number of compute cores

used for each simulation varies from 8 cores for a system of 800 atoms to 128 cores for a system of 160,000 atoms. The total compute time for each MD simulation on LAMMPS is between 12 to 48 hours.

Chapter 2 gives a brief introduction to MD simulations. In section 2.1, all pre-simulation steps will be addressed, such as the initial position and velocity of each atom of the system, the application of the boundary conditions, the choice of an inter-atomic potential, and the creation of the LAMMPS input files. In section 2.2, the simulation procedure will be detailed. A brief overview of the most widely used methods for the computation of the thermal conductivity will first be presented. Then, each step of the simulation will be explained. Section 2.3 will explain the post-treatment of the results after an EMD simulation based on the Green-Kubo method.

Chapter 3 is a paper that we published in the proceedings of the 2nd International Conference on Nanotechnology: Fundamentals and Applications (2011). It is an introduction to the effects of the post-treatment of MD simulations on the calculation of the thermal conductivity of CNTs. Only a 5 nm long nanotube is studied in this paper. The next paper presented in Chapter 4 has been submitted for publication in the Journal of Computational Physics and is a continuation of the preceding chapter. It presents the study of the effects of post-treatment parameters on the thermal conductivity for CNTs of different lengths. This paper is focused on the use of a double-exponential best-fit of the auto-correlation function that is frequently used in literature for EMD simulations based on the Green-Kubo method. Also, the necessity to use early time best-fit of the auto-correlation function is questioned. Finally, Chapter 5 presents a short paper that will be submitted for publication in Applied Physics Letters. It addresses the exact role of the frequency cut-off in carbon nanotubes and compares the importance of this phenomenon to other parameters that can influence the calculated thermal conductivity when performing EMD simulations with the Green-Kubo method.

CHAPTER 2: Introduction to molecular dynamics simulations

Classical molecular dynamics is a numerical tool used to get insights of the physics at a molecular level. It is based on solving the equations of motion (Newton's second law) in order to calculate the transient evolution of the position and velocity of each atom of a system. MD simulations can model phonon-phonon interactions, but it can neither model phonon-electron nor electron-electron interactions. However, the electron contribution to the thermal conductivity of carbon nanotubes can be considered negligible [13]. For this reason, the thermal conductivity obtained from a MD simulation is often referred to as the lattice thermal conductivity. The interactions between the atoms during a simulation are governed by an inter-atomic potential. Different types of potentials can be used to act as the driving forces. The choice of the inter-atomic potential is a crucial step in the simulation procedure, since it has to represent properly both the microscopic and macroscopic properties of the simulated materials. However, choosing an inter-atomic potential is only one step amongst many towards running a complete molecular dynamics simulation. The latter is usually divided into 3 distinct parts: pre-simulation, simulation, and post-treatment. Each of these parts is detailed in the following sections.

2.1 PRE-SIMULATION

Initial position

Before running a simulation, the initial and boundary conditions of the problem have to be established. One must first decide of the chirality and the length of the carbon nanotube. With the (n, m) indices of the chiral vector and the length of the tangential vector, it is possible to calculate the initial position of all the atoms of the carbon nanotube. One can notice that the length of the tangential vector $\vec{T}$ corresponds to the length L of the carbon nanotube and the length of the chiral vector $\vec{C}_h$ corresponds to the circumference of the nanotube. Using this, it is possible to express those vectors in the following manner:

$$\bar{C}_h = \pi d \cos\theta \hat{e}_x - \pi d \sin\theta \hat{e}_y \tag{2.1}$$

$$\bar{T} = L \sin\theta \hat{e}_x + L \cos\theta \hat{e}_y \tag{2.2}$$

where $\hat{e}_x$ and $\hat{e}_y$ are unit vectors in the (x, y) referential. Another useful referential is now defined, the (1, 2) referential, with unit vectors $\hat{e}_1$ and $\hat{e}_2$. See Fig. 1.4 for a visual representation of those two systems of coordinates. The boundaries of the grey box in the (x, y) referential are given by:

$$[x_{min},\ x_{max}] = [0,\ \pi d \cos\theta + L \sin\theta] \tag{2.3}$$

$$[y_{min},\ y_{max}] = [-\pi d \sin\theta,\ L \cos\theta] \tag{2.4}$$

A MATLAB routine has been written to calculate the position of all atoms included within those boundaries. The atoms coordinates are then transferred in the (1, 2) referential. In order to convert (x, y) coordinates to (1, 2) coordinates, the following rotation tensor is used (with θ positive counter-clockwise):

$$\begin{bmatrix} x_1 \\ y_2 \end{bmatrix} = \begin{bmatrix} \cos\theta & \sin\theta \\ -\sin\theta & \cos\theta \end{bmatrix} \begin{bmatrix} x \\ y \end{bmatrix} \tag{2.5}$$

Once the atoms coordinates are known in the (1, 2) referential, all atoms within the carbon nanotube boundaries, i.e. within the grey box whose limits are [0 , πd] and [0 , L] in the (1, 2) referential, are said to belong to the CNT. Only those atoms shall be used in the construction of the CNT. To avoid atom superposition when the three dimensional CNT is constructed (when the two-dimensional graphite sheet is wrapped into a cylinder), atoms on the $x_1 = \pi d$ boundary are excluded from the CNT. Finally, each atom is given a position in the three dimensional space to create the real CNT using the (X, Y, Z) coordinate system, as illustrated in Fig. 2.11.

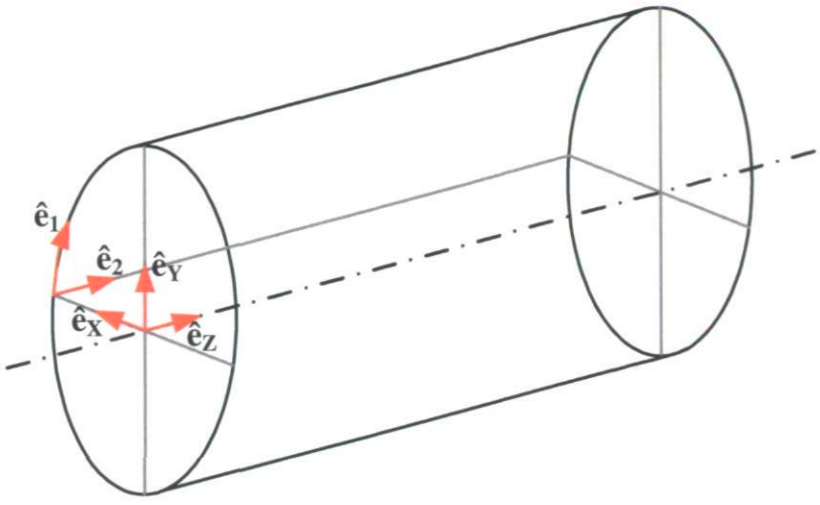

Figure 2.11: Coordinate system conversion from (1, 2) to (X, Y, Z) referential

where $\hat{e}_X$, $\hat{e}_Y$, and $\hat{e}_Z$ are unit vectors in the (X, Y, Z) referential. The coordinates of all the atoms in the (X, Y, Z) referential are thus obtained from:

$$X = \frac{d}{2}\cos\left(\frac{2}{d}x_1\right) \tag{2.6}$$

$$Y = \frac{d}{2}\sin\left(\frac{2}{d}x_1\right) \tag{2.7}$$

$$Z = y_2 \tag{2.8}$$

The Z coordinate of all the atoms of the system are finally shifted by a distance L/2 so that the CNT's center of mass is at the origin of the (X, Y, Z) referential. The complete MATLAB routine calculates the (X, Y, Z) coordinates of all N atoms of the system for a given (n, m) chiral vector, a given L, and a given lattice constant a. To ensure that the routine works properly, the diameter of a (10, 10) CNT obtained has been compared to its theoretical value. Furthermore, the total number of atoms N of the CNT has been compared to the number of atoms reported for the same type of CNT in [11] for different values of L. The results of the validation of the MATLAB routine are given in the following table.

Table 2.1: Validation of the three-dimensional CNT construction with MATLAB routine

Length of CNT [nm]	$N_{[11]}$* [atoms]	N_{MATLAB}* [atoms]	$d_{theoretical}$ [Å]	d_{MATLAB} [Å]
4.92	800	800	13.563	13.563
9.84	1600	1600	13.563	13.563
19.68	3200	3200	13.563	13.563
39.36	6400	6400	13.563	13.563

* Total number of atoms obtained from a CNT with periodic boundary conditions

Initial velocity

The next pre-simulation step is to determine the initial velocity distribution of the system. There are usually two ways of attributing a velocity to each atom. The first one consists of randomly sampling the magnitude of the velocity vector of each atom from the Maxwell-Boltzmann distribution at a given temperature, which is the equilibrium distribution for such systems [16]. A direction is then randomly attributed to each of the velocity vectors. Since the MATLAB *rand* function that is used samples numbers in the interval [0, 1] according to a uniform probability density function (PDF), a mapping of the obtained values is necessary to find corresponding velocities that respect the Maxwell-Boltzmann distribution. Let f(x) be the uniform PDF of the *rand* function. Then, f(x)dx is the probability that a number x sampled from this distribution is comprised between x and x + dx. Integrating f(x) from x = 0 to x = X gives the probability that a number x is comprised in the interval [0, X]. The resulting function, F(x) is called the cumulative distribution function (CDF) of the uniform distribution. The integral of f(x) from x = 0 to x = 1 is equal to one, since there is 100% chance that a number given by the *rand* function is in the interval [0, 1]. In the same manner, let f(v) be the Maxwell-Boltzmann PDF. The integral of f(v) from v = 0 to v = V gives the probability that a velocity v is comprised in the interval [0, V]. Thus, one can obtain the Maxwell-Boltzmann CDF, F(v), by integrating f(v). In order to obtain a mapping from f(x) into f(v), one must seek the value V by integrating f(v) on the interval [0, V] that gives the same probability as the integral of f(x) on the interval [0, X], where X is randomly given by the *rand* function. In other words, one must find the value V for

which F(X) = X = F(V). Mathematically, this procedure is given by the following equations:

$$\int_0^{V_i} f(v)dv = X_i \tag{2.9}$$

with the following normalized probability density function:

$$f(v) = \sqrt{\frac{2}{\pi}} \frac{v^2}{\alpha^3} e^{-v^2/(2\alpha^2)} \tag{2.10}$$

where the distribution parameter is given by:

$$\alpha = \sqrt{\frac{k_B T_{MD}}{M_i}} \tag{2.11}$$

In the preceding equation, T_{MD} is the desired temperature of the MD simulation and M is the mass of the atoms. The subscript i refers to the i^{th} atom of the system. Thus, this procedure is repeated for each atom to get the initial magnitude of their velocity vector. The small circle in Fig. 2.12 is an example of a random point sampled from the uniform PDF (bottom left) with a corresponding probability F(X) using the CDF (top left). This probability must be the same as the one given by the Maxwell-Boltzmann CDF (top right). The velocity V is then found by integrating numerically the Maxwell-Boltzmann PDF (bottom right) until F(V) = F(X).

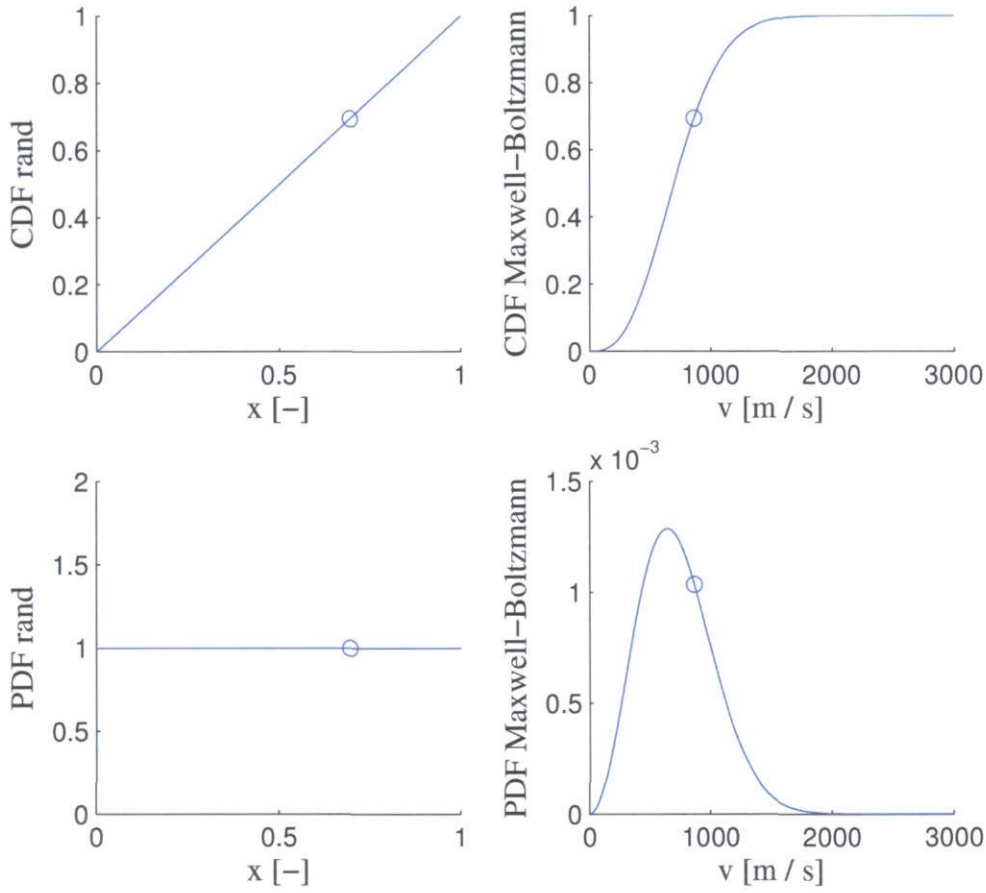

Figure 2.12: Uniform and Maxwell-Boltzmann PDF and CDF

The second way of determining the initial velocity of the atoms is to use the fact that the Maxwell-Boltzmann distribution allows the use of the equipartition theorem to evaluate the kinetic energy E_K of the system in the following manner:

$$E_K = \sum_{i=1}^{N} \frac{1}{2} M_i v_i^2 = \frac{3}{2} N k_B T_{MD} \tag{2.12}$$

If one takes the same magnitude of the initial velocity vector and the same mass for all the atoms of the system, then the initial velocity of all the atoms is given by:

$$v_i = \sqrt{\frac{3k_B T_{MD}}{M}} \tag{2.13}$$

The directions of all the velocity vectors are then randomly distributed in space. If the system is allowed to evolve freely from this point, it will eventually reach an equilibrium state with a Maxwell-Boltzmann velocity distribution. The validity of Eq. (2.12), however, depends on certain conditions [17]: (1) there must be no temperature constraint on the system that can perturb the Maxwell-Boltzmann distribution, (2) the total momentum of the system must be zero, and (3) the heat capacity must be independent of temperature, which is only valid if T_{MD} is greater than the Debye temperature. For temperatures below the Debye temperature, which is much higher than room temperature, there are quantum effects that are completely neglected when using classical MD simulations.

Once the velocity vectors of all the atoms of the system have been initialized, it is required to minimize both the total linear and angular momenta of the system. This step is necessary to ensure that the CNT does not have any translational or rotational motion in space. The procedure used to do this has been suggested by [11]. The center of mass (CM) velocity $\vec{V}_{cm}$ is first calculated and removed in the following manner:

$$\vec{v}_i = \vec{v}_i - \vec{V}_{cm} \tag{2.14}$$

This procedure assures that the both the initial center of mass velocity and linear momentum $\vec{P}$ of the system are zero. The position vector $\vec{r}_i$ of each atom is then calculated with respect to the CM position of the system. Once this is done, the angular momentum $\vec{L}$ of the system is calculated with:

$$\vec{L} = \vec{R}_{cm} \times M\vec{V}_{cm} + \sum_{i=1}^{N} m_i \left(\vec{r}_i \times \vec{v}_i\right) \tag{2.15}$$

where $\vec{R}_{cm}$ is the position of the center of mass and M is the total mass of the system. The first term on the RHS of Eq. (2.15) disappears since the center of mass velocity is zero. The angular velocity $\vec{\omega}$ of the system is now required to remove the rotational motion of the CNT. One can express the angular momentum as a linear transformation of the angular velocity of the system [18] by using the moment of inertia tensor I:

$$\vec{L} = I\vec{\omega} \tag{2.16}$$

The moment of inertia coefficients are given by:

$$I_{jk} = \sum_{i=1}^{N} M\left(r_i^2 \delta_{jk} - r_{j,i} r_{k,i}\right) \tag{2.17}$$

where δ_{jk} is the Kronecker delta. Both j and k in the preceding equation can take the values of X, Y, or Z. The components of the position vector $\vec{r}_i$ in the (X, Y, Z) referential are thus denoted by $r_{X,i}$, $r_{Y,i}$, and $r_{Z,i}$, while its modulus is denoted by r_i. Once the moment of inertia tensor has been calculated, the angular velocity $\vec{\omega}$ is obtained by inverting Eq. (2.16) and the rotational motion of the CNT is removed by applying the equation that follows:

$$\vec{v}_i = \vec{v}_i - \vec{\omega} \times \vec{r}_i \tag{2.18}$$

Removing the translational and rotational motion of the CNT will slightly modify the temperature of the system. Modifying the velocity of each atom results in a variation of the total kinetic energy of the system, which can be related to the temperature of the system, as was explained before. This slight variation is not relevant, however, since as will be discussed in the simulation section, the temperature of the system will be further modified to be brought back to the desired T_{MD}.

Boundary conditions

There are typically three types of boundary conditions that can be used in MD simulations of carbon nanotubes: periodic boundary condition (PBC), free boundary condition, and fixed boundary condition. Since fixed and free boundary conditions are straightforward and because they are not used in the present work, they will only be explained briefly. For fixed boundary conditions, the atoms at both ends of the CNT are fixed in space (zero velocity) for all the simulation. The use of fixed boundary conditions renders the removal of the translational and rotational motion of the nanotube unnecessary, since the fixed ends will prevent any such motion. For free boundary conditions, no restriction of any kind is applied on the atoms of the nanotube. The atoms are allowed to move freely from their initial condition. It is thus important that the CNT have no total momentum (zero linear and angular momenta) since the nanotube must not rotate or move in a manner that it exits the simulation domain. When using fixed or free boundary conditions, additional phonon scattering will occur at both ends of the nanotube. This is why those two boundary conditions are usually used when one wishes to study the finite length effects on the properties of nanotubes.

Periodic boundary condition, however, is meant to emulate an infinite size nanotube without having to use an infinite number of atoms. It is equivalent to filling the entire space with identical copies of the simulation domain (see Fig. 2.13). The number of such copies is limited by the fact that the interactions between the atoms, modeled by the inter-atomic potential, have a finite range, or a cut-off range, beyond which the interactions are assumed to be negligible. If an atom crosses a periodic boundary, it will reenter the simulation domain through the opposite boundary.

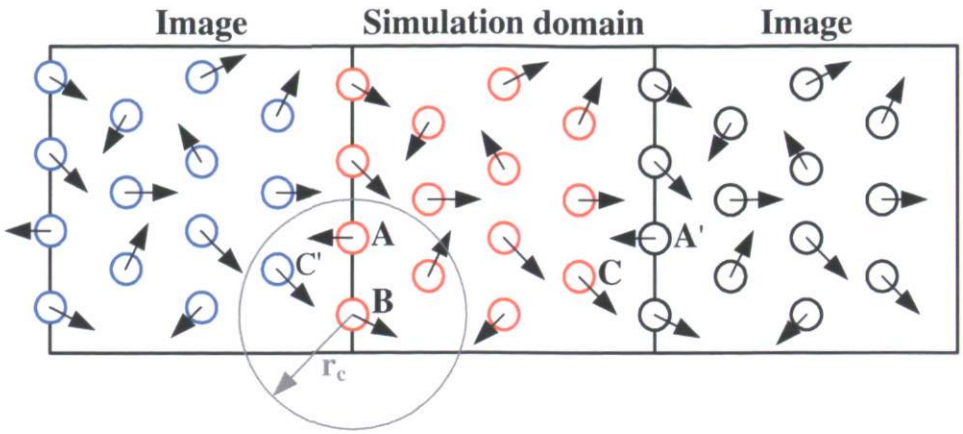

Figure 2.13: Schematic representation of periodic boundary condition

Many features of the periodic boundary condition are represented in Fig. 2.13. The simulation domain represented in this figure can be seen as the initial set-up of a two-dimensional MD simulation of carbon atoms in graphite. Only the left and right images have been represented, but other images exist at top, bottom, and four corners of the simulation domain. One can first notice that the images are not mirror images of the simulation domain, but translations. In order to avoid the superimposition of atoms (and huge, unphysical repulsive forces) at the beginning of the simulation, care must be taken in removing all the atoms that are on the right (or left) boundary. Those atoms will still exist in the images of the simulation domain. When using PBC, this step is done prior to the attribution of the initial velocity of the atoms. One can also see an example of an atom crossing a periodic boundary. When atom A crosses the left boundary, its image A' immediately reenters through the opposite boundary and conserves its momentum. Fig. 2.13 also shows how the cut-off length r_c of the inter-atomic potential influences the interaction between atoms when using PBC. Atom B is too far from atom C in the simulation domain and therefore, cannot interact with it. However, atom B is close enough to atom C' in the left image to interact with it.

Even though PBC is meant to represent a system of infinite size, there are still issues to be addressed which can cause finite size effects even when using PBC. Those length effects are explained in [17] and will be addressed in the post-simulation section of this chapter.

Inter-atomic potential

The inter-atomic potential dictates how the atoms or molecules of a system interact with each other. The force $\vec{F}_i$ acting on the atom i can be obtained by taking the gradient of the total potential φ of the system:

$$\vec{F}_i = -\frac{d\varphi}{d\vec{r}_i} \tag{2.19}$$

The total potential of the system can be expressed as the sum of pair potentials φ_{ij}:

$$\varphi = \frac{1}{2}\sum_{i=1}^{N}\sum_{\substack{j=1 \\ j\neq i}}^{N}\varphi_{ij} \tag{2.20}$$

where the 1/2 factor has been included to avoid adding twice the contribution of each pair of atoms to the total potential energy. The majority of the potentials are empirical or semi-empirical. They are based on mathematical models with unknown parameters that have been fitted so that the MD results match some experimentally measured physical properties of the matter, such as the melting point, the elastic constant, the lattice constant, and so on [16]. Some of them can be expressed rather simply, with a few numbers of parameters, such as the well-known Lennard-Jones (LJ) potential:

$$\varphi_{ij} = 4\varepsilon\left[\left(\frac{\sigma}{r_{ij}}\right)^{12} - \left(\frac{\sigma}{r_{ij}}\right)^{6}\right] \tag{2.21}$$

The two parameters, ε and σ, represent the depth of the potential well (minimum value of the potential) and the distance at which the inter-atomic potential is zero, respectively. The potential takes the value of ε when the distance between the two atoms is $2^{1/6}\sigma$. The first term of the LJ potential represents the short-range, repulsive force between two atoms, while the last term represents the long-range, attractive force. To represent systems made of carbon atoms such as carbon nanotubes, more sophisticated potentials must be used. The Tersoff [19-20], REBO [21-23], and AIREBO [24] potentials are

examples of inter-atomic potentials that have been widely used for simulation of carbon systems. These potentials all contain modified pair potential terms that take into account the effect of a given atom on the interaction of two other atoms. These interactions are called three-body interactions. They also display many more complex features that will not be detailed here, but an interested reader is invited to consult the suggested references.

LAMMPS input files

All the MD simulations presented here have been performed with the open-source LAMMPS (Large-scale Atomic/Molecular Massively Parallel Simulator) software. An up-to-date version of this software can be downloaded at http://lammps.sandia.gov/. In order to perform a simulation with this software, input files must first be created. This is the last test of the pre-simulation procedure.

The first and most important file is the **simulation.txt file**. It contains a list of LAMMPS commands that will be executed by the software to perform the simulation. For a complete description of all the LAMMPS commands and input files structure, a full version of the LAMMPS user's manual can be found on the previously given website. An example of such simulation file is given in Appendix 1. This sample simulation file has been made for an equilibrium molecular dynamics (EMD) simulation of a 1000 nm long carbon nanotube with periodic boundary conditions. Note that the axial component of the heat flux is calculated at each time step and written in output files. The use of these output files will be discussed in the post-treatment section of this chapter. One can notice that a read_data command is used in the simulation set-up part. Once executed, this command will read the initial atom data of the simulation from another input file, the **atomData.txt file**. This file contains the following information: number of atoms, atom types, boundaries of the simulation domain, initial position and type of each atom, initial velocity of each atom, and atomic mass of each type of atom. The units of the written data must be the same as those specified in the simulation.txt file. In all the simulations, the units metal are used.

2.2 SIMULATION

Types of simulation

The two types of simulation used most frequently are equilibrium molecular dynamics (EMD) and non-equilibrium molecular dynamics (NEMD) simulations. Both methods can be used for the calculation of thermal conductivity of carbon nanotubes and require very different simulation set-up.

EMD simulations consist in the calculation of the position and the velocity of each atom in an equilibrium system. A system is considered to be in an equilibrium state if the velocity distribution of the atoms corresponds to a Maxwell-Boltzmann distribution and if the total energy of the system is constant in time. In MD simulation language, an equilibrium run can be called a NVE run, i.e. a simulation with constant number of atoms (N), volume (V), and energy (E). The thermal conductivity of the system is then calculated on the basis of the linear response theory [16]. The details of the calculation of the thermal conductivity for EMD simulations are given in the next section of the current chapter. Since most of the time the initial velocity distribution of the system does not correspond to a Maxwell-Boltzmann distribution, an equilibration run (NVE) must first be done. Then, a NVT run is done to bring the system to the desired temperature. This is a simulation with constant number of atoms (N), volume (V), and temperature (T). Finally, another NVE run is performed during which the axial component of the heat current and the mean temperature of the system at each time step are calculated and written in output files. This data will be used during the post-treatment to calculate the thermal conductivity.

NEMD simulations differ from EMD simulations in that the system simulated is not in an equilibrium state. A thermal gradient is introduced in the system by adding a hot and a cold reservoir at each end of the carbon nanotube, as shown in Fig. 2.14. Those reservoirs are kept at constant temperature by adding energy in the hot reservoir and removing energy in the cold reservoir at each time step. Once the system has reached a steady-state, the temperature profile of the carbon nanotube is calculated and the thermal conductivity is obtained from Fourier's law of conduction. The thermal gradient introduced in the

system during NEMD simulations can reach values typically around 10^{10} K/m (difference of 50K in a 5 nm long nanotube), which is physically impossible. That is why we chose to use the EMD method instead of the NEMD method.

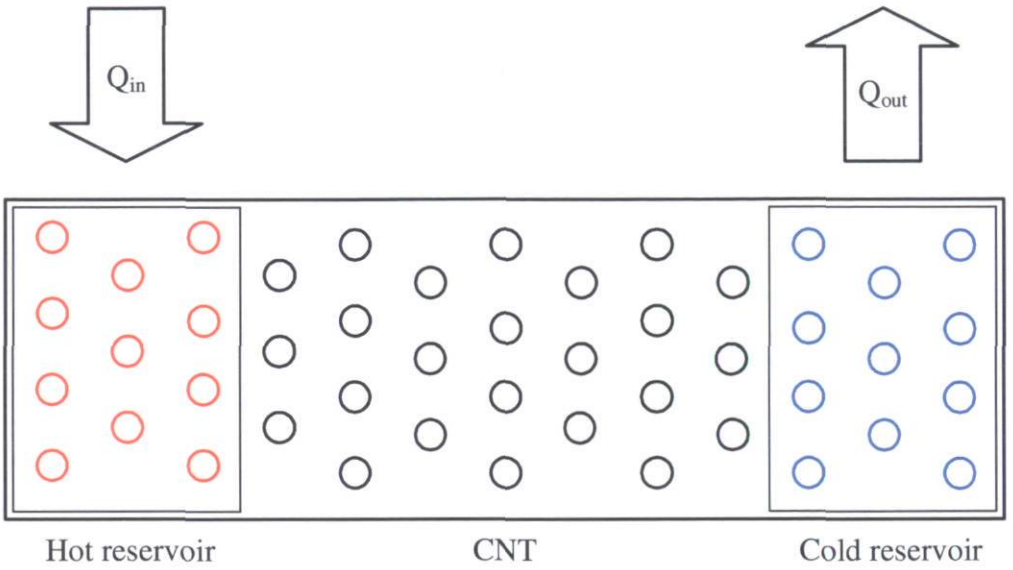

Figure 2.14: Schematic representation of a typical system for NEMD simulations

Validation of the EMD simulation procedure

Before performing any simulation, a validation of the EMD simulation procedure is required. As explained in the previous section, an equilibration run is necessary to bring the system to an equilibrium state. The equilibration run has to be long enough to allow the system to reach equilibrium. To determine the correct time of the equilibration run (number of time steps), a NVE simulation is performed for a 10 nm long (10, 10) CNT (1,600 atoms) using the REBO potential. The positions of the atoms are initialized as explained previously. The initial velocity distribution of the system is uniform at a mean temperature of 300K. The time of the NVE run has been chosen as 100,000 time steps of 0.001 ps. After this equilibration run, a NVE run of 100 more time steps has been done during which the velocity of each atom and the mean temperature of the system have been written in output files. The velocity distribution has been calculated at each time step and averaged over the 100 time steps. To do this, the velocity axis is separated in intervals of 100 m/s and the number of atoms within each interval is calculated and averaged over the 100 time steps. The average velocity distribution is finally normalized

so that its maximum value matches the maximum value of the theoretical distribution. The Maxwell-Boltzmann velocity distribution has also been calculated at a temperature matching the temperature of the simulation during these 100 time steps, which corresponds approximately to a mean temperature of 180K. Even though the temperature of the system decreases, it will be brought back to the desired temperature during the NVT run. The average velocity distribution of the simulation and the theoretical velocity distribution are both shown in the next figure. Since both velocity distributions are essentially the same, it can be concluded that the chosen number of time steps of the equilibration run is long enough to allow the system to reach an equilibrium state.

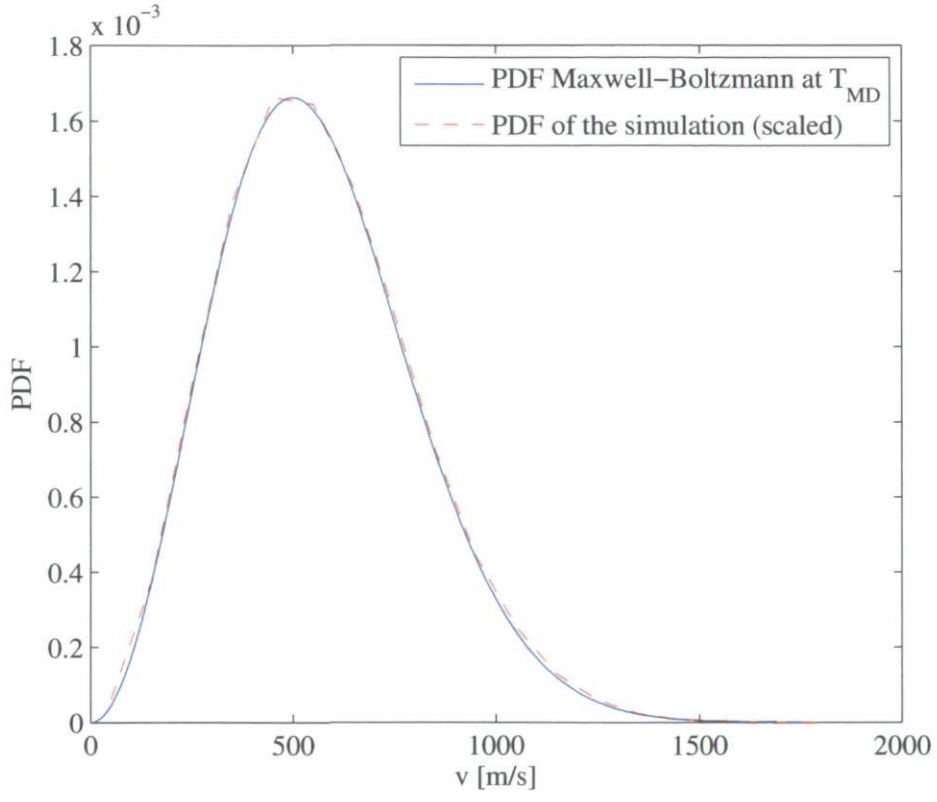

Figure 2.15: Velocity distribution after the equilibration run

It has been said that the mean temperature of the system was approximately 180K, even if it was initially 300K. Since the total energy of the system is constant, a drop in temperature means that a portion of the kinetic energy of the system has been converted

into potential energy. If the bond between two atoms is modeled by a spring, the potential energy stored within the spring will increase if it is compressed. Using this analogy, the increase of potential energy of the system means that the atoms have been brought closer to each other and that the mean radius of the carbon nanotube has decreased. The mean radius of the carbon nanotube during the equilibration run has been calculated and averaged over the first 25,000 time steps. As expected, the mean radius of the carbon nanotube decreases from the initial theoretical value of 6.7813 Å to a value of approximately 6.6686 Å. This represents a decrease in radius of less than two percent. The reasons for this change in radius have not been studied in detail, but the mean radius has been found to be dependant of the inter-atomic potential used in the simulation.

The second step of an EMD simulation is the NVT run which allows the system to reach a desired temperature. There exists different methods to do so, but LAMMPS uses the Nosé-Hoover thermostat. The temperature of the system has been calculated during a typical simulation. The simulation consisted in a 100,000 time steps NVE run for equilibration, a 400,000 time steps NVT run to bring the system to a mean temperature of 300 K, and a 1,000,000 time steps NVE run. The mean temperature of the system as a function of time during a simulation can be seen in the next figure.

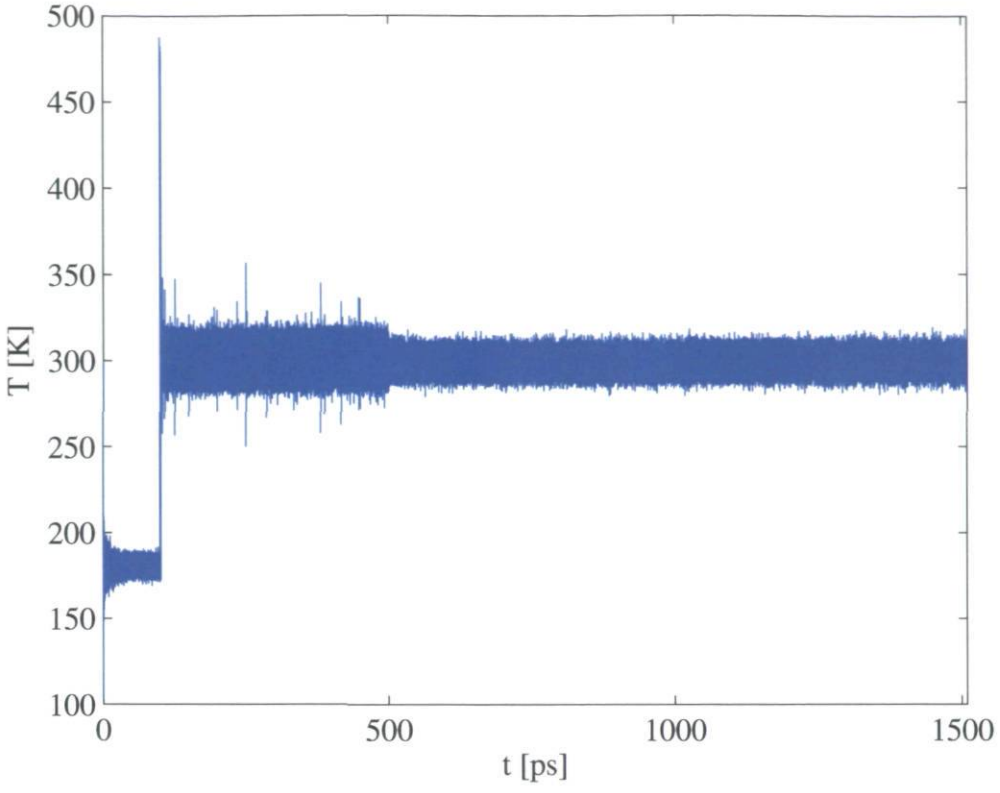

Figure 2.16: Mean temperature of the system during a simulation

Each of the three simulation parts can be seen in Fig. 2.16: the equilibration run where the mean temperature is 180K, the NVT run where the temperature of the system is brought back to 300 K, and the NVE run where the mean temperature remains at 300 K but with smaller oscillations. This means that the chosen number of time steps of the NVT run is large enough to allow the system to reach and remain at the desired temperature during a simulation.

Validation of the minimization of the initial total momentum of the system

The procedure for the minimization of the initial linear and angular momenta has been explained in section 2.1. It is required to validate this procedure and to verify that the zero total momentum of the system is well preserved during a simulation. A MATLAB routine has been written to calculate: (1) the position of the center of mass, (2) the velocity of the center of mass, (3) the linear momentum of the system, and (4) the angular

momentum of the system. The required data is the positions and velocities of all the atoms at each time step of the simulation.

Two test cases have been considered to validate the MATLAB routine. For the first test case, a 5 nm long (5, 5) carbon nanotube (400 atoms) with all atoms moving in the same direction at the most probable velocity of the Maxwell-Boltzmann distribution at 180 K, which corresponds approximately to a velocity of 500 m/s, is considered. The linear momentum of the system is given by:

$$\vec{P} = \sum_{i=1}^{N} m_i \vec{v}_i \tag{2.22}$$

For a nanotube made of carbon atoms with a velocity of 500 m/s, the theoretical value of the linear momentum is $\left|\vec{P}\right| = 4.9793$ (eV/Å) ps. Since all the atoms are moving in the same direction, the angular momentum of the system is expected to be zero.

For the second test case, a 5 nm long (5, 5) carbon nanotube rotating about its axis at a tangential velocity corresponding the most probable velocity of the Maxwell-Boltzmann distribution at 180 K is considered. The linear momentum of the system is expected to be zero. The angular momentum of the system is calculated using Eq. (2.15), which simplifies to the following equation when the center of mass velocity is zero:

$$\vec{L} = \sum_{i=1}^{N} m_i \left(\vec{r}_i \times \vec{v}_i\right) \tag{2.23}$$

Again, for a nanotube made of carbon atoms with a tangential velocity of 500 m/s, the theoretical value of the angular momentum is $L_z = 16.8831$ eV ps. Since the nanotube is rotating about its axis, the x and y components of the angular momentum are expected to be zero. For both test cases, the calculated values of the linear and angular momenta using the MATLAB routines match the theoretical values.

Conservation of the linear and angular momenta during a simulation

To verify that the zero linear and angular momenta are conserved during a simulation, a NVE run has been performed for a 5 nm long (10, 10) CNT using the REBO potential. The simulation time is 10,000 time steps of 0.001 ps. The MATLAB routine has been used to calculate the properties of the system, i.e. center of mass position and velocity, linear momentum, and angular momentum. The units used in the following figures are the same as those of a simulation in LAMMPS. Because the simulation data is written in LAMMPS input and output files using a 15 digits exponential format, the center of mass position and velocity cannot be exactly zero. Moreover, there is a finite numerical precision for all variables and a propagation of errors (round off errors) during a simulation.

The order of magnitude of the x and y components of the position (top and middle left) and of all the components of the velocity (right, from top to bottom) of the center of mass in Fig. 2.17 can be explained by these reasons. However, the large variations in the z component of the center of mass position (bottom left) can be attributed to the initial position of the boundary conditions (see Fig. 2.13). Using this set-up in the axial direction and assuming that z = 0 lies in the middle of the simulation domain, the initial z component of the center of mass will be slightly smaller than zero, but of the order of magnitude of 1 Å. Once the simulation is started, the atoms lying on the left PBC can cross the boundary back and forth, which results in variations of the z component of the center of mass position.

As can be seen in Fig. 2.18, the same conclusions can be drawn for the components of the linear (left) and angular (right) momentum of the system. There is some concern with the x and y components of the angular momentum. The large value of those components could be caused by the vibration modes of the carbon nanotube. As the nanotube experiences a combination of radial, longitudinal and tangential vibrations, it deforms in such a manner that the instantaneous angular momentum is not zero about these axes. This could make the angular momentum quite large at a given time step, without being larger than the value calculated in the second test case. What matters the most is that the

mean value of the components of the angular momentum is zero during the simulation, which is the case.

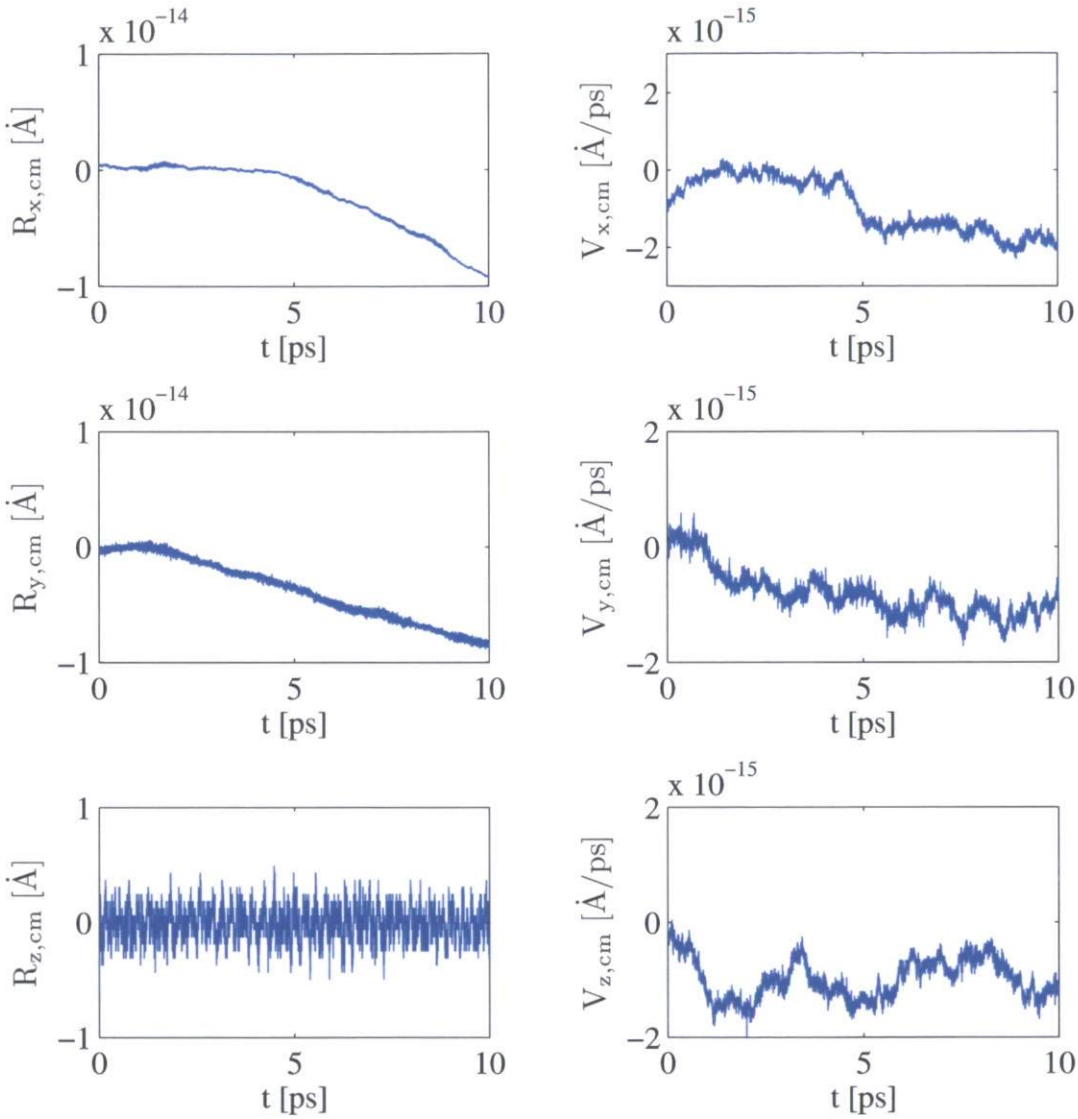

Figure 2.17: Preservation of the center of mass position and zero velocity

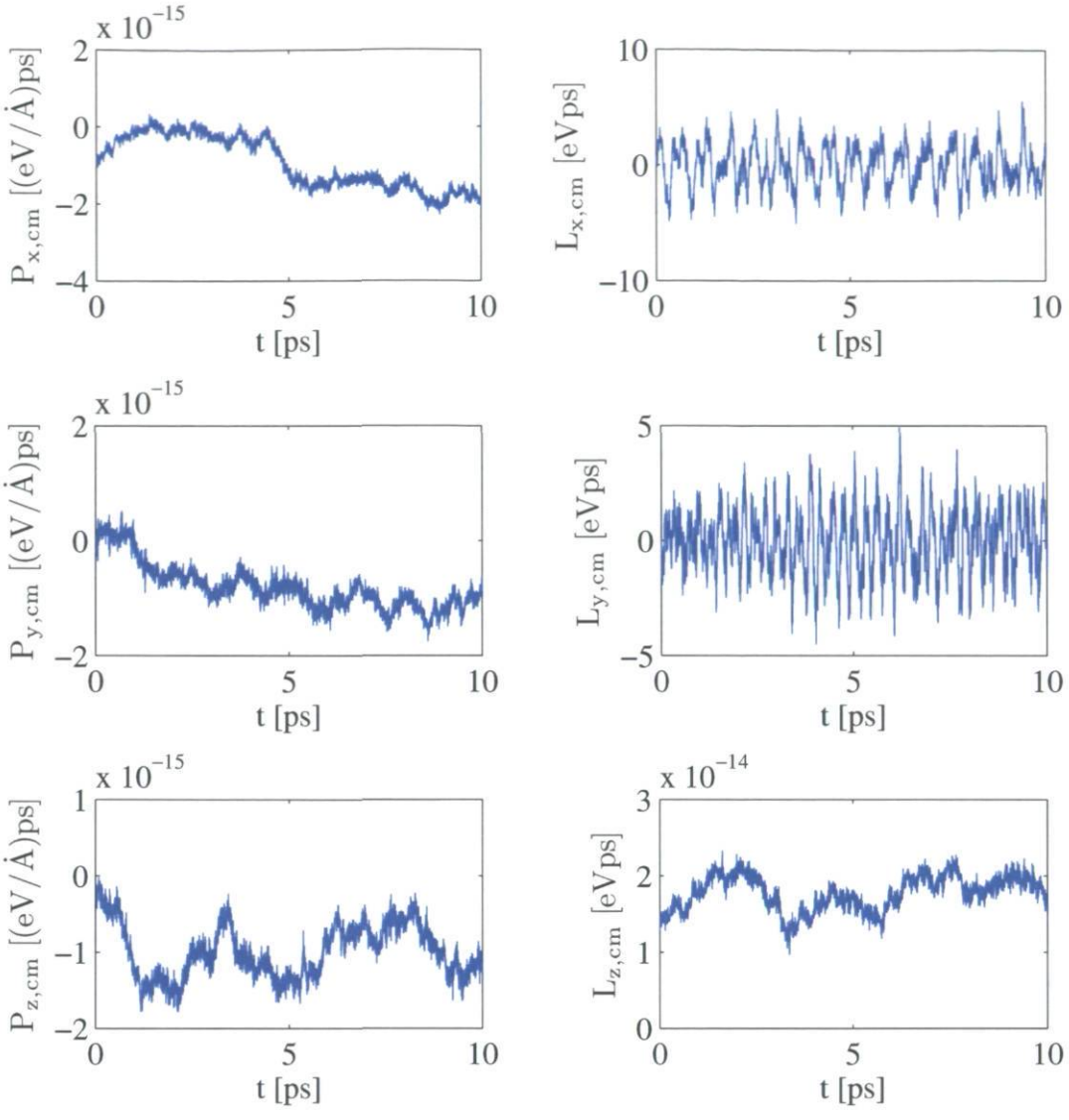

Figure 2.18: Preservation of the zero total momentum of the system

The same verification has been done at the end of a typical simulation. The simulation is the same as the one for the validation of the NVT run. At the end of this simulation, an additional NVE run of 10,000 time steps has been performed during which the position, velocity, linear and angular momentum of the system have been calculated. The results can be seen in Figs. 2.19 (left: position and right: velocity) and 2.20 (left: linear and right: angular momentum).

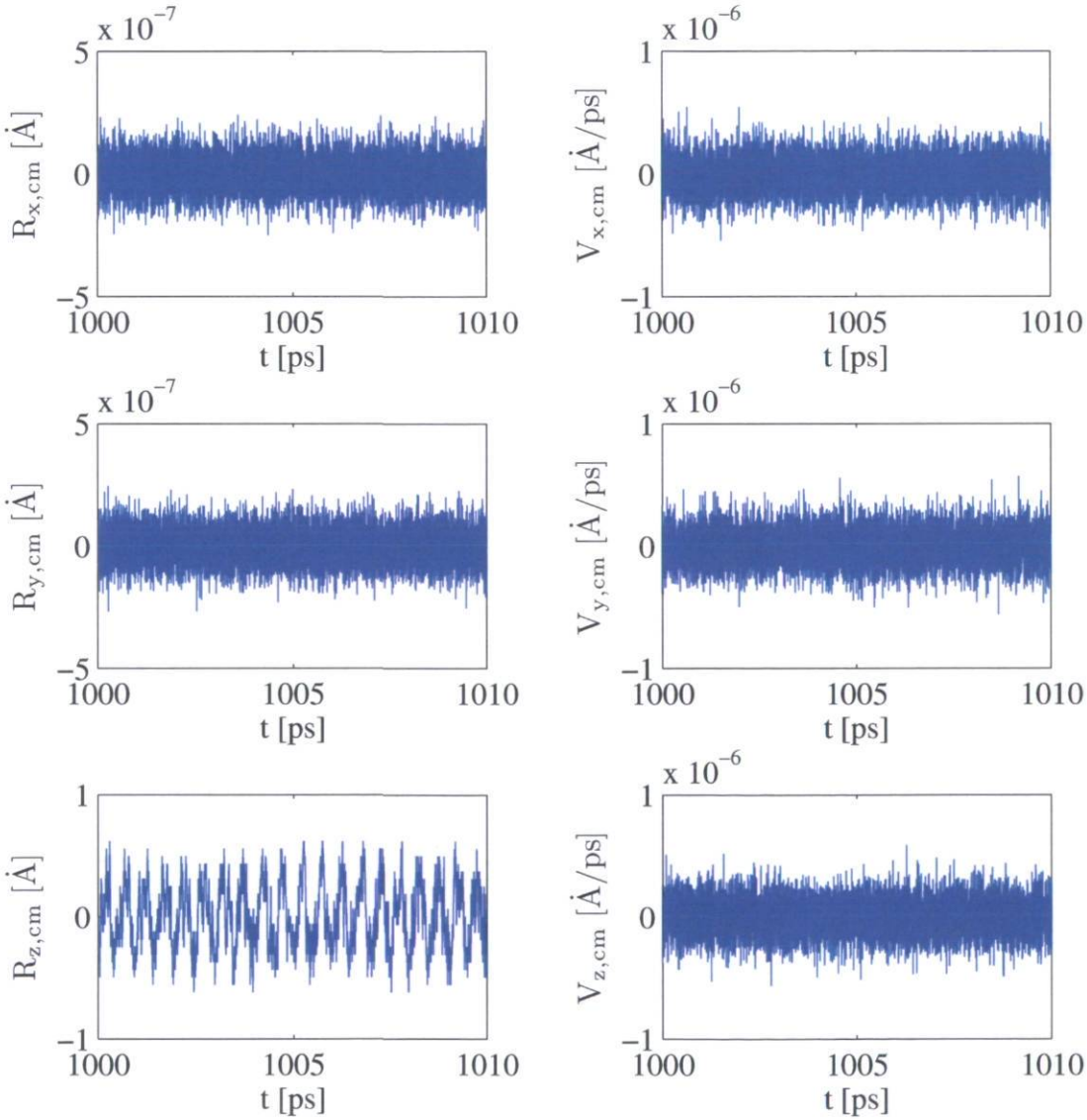

Figure 2.19: Center of mass position and velocity at the end of a simulation

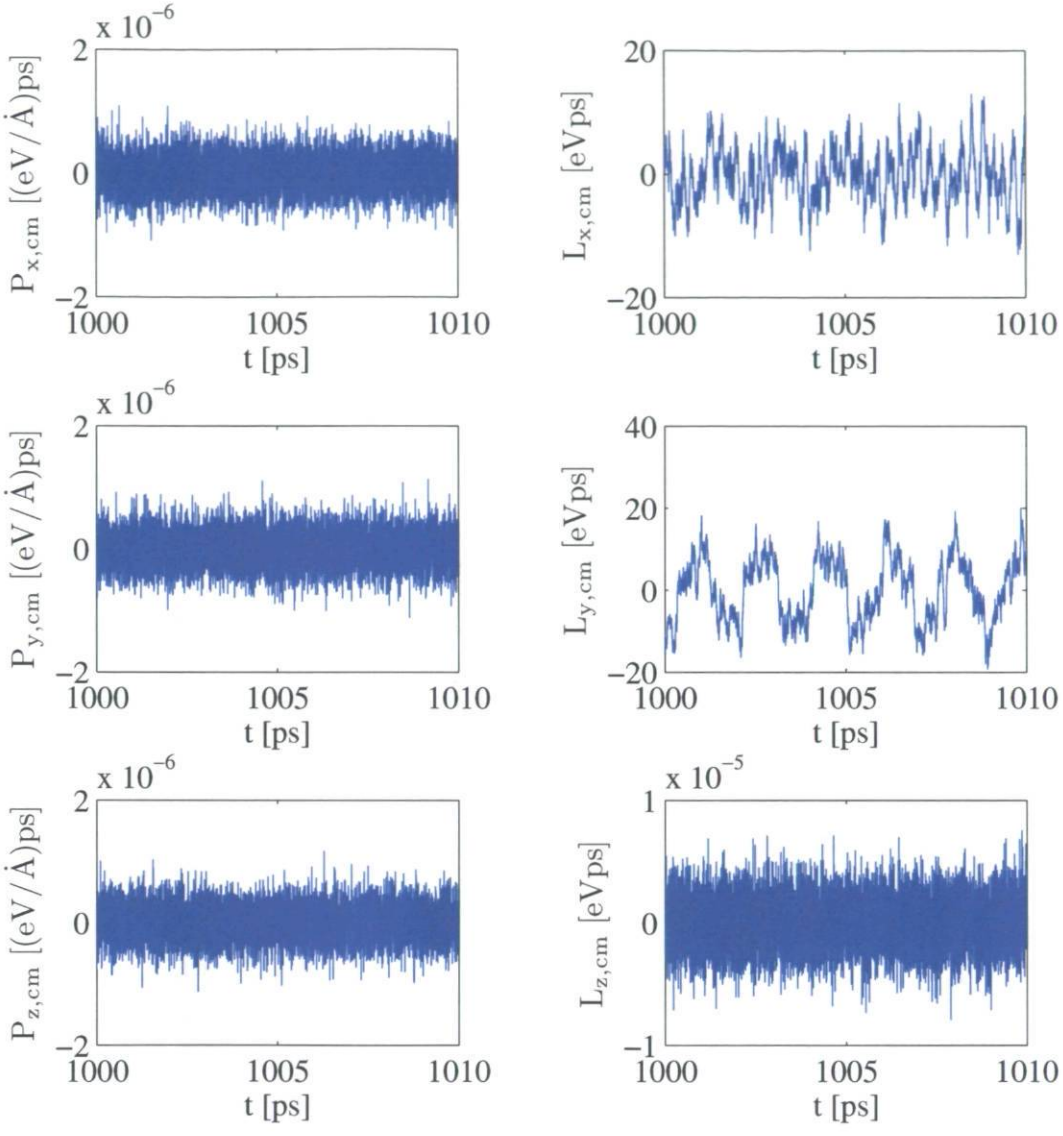

Figure 2.20: Zero total momentum of the system at the end of a simulation

The order of magnitude of all these variables has increased and stabilized during the simulation. However, it remains negligible compared to the order of magnitude of the simulation variables. It can thus be concluded that the position and velocity of the center of mass, the zero linear momentum, and the zero angular momentum are well preserved during a simulation.

2.3 POST-TREATMENT

At the end of an EMD simulation, the available data consists in the axial component of the heat current (the compute heat/flux command on LAMMPS computes the heat current, not the heat flux) and the mean temperature of the system at every time step. It is possible to use this data to calculate the lattice thermal conductivity of a carbon nanotube using the following equation, which can be derived from the linear response theory [16]:

$$k = \frac{1}{k_B T_{MD}^2 LA} \int_0^\infty \left\langle j_z(0)\, j_z(t) \right\rangle dt \tag{2.24}$$

where k_B is the Boltzmann constant, T_{MD} is the temperature of the system (taken as the average of the mean temperature of the system during the simulation), L and A are the length and cross-sectional area of the nanotube, and j_z is the axial component of the heat current. There are different conventions for the cross-sectional area of a nanotube, but the one used in all simulations of the present work is a ring with a thickness equal to 3.4 Å. In Eq. (2.24), $\left\langle j_z(0)\, j_z(t) \right\rangle$ is called the heat current auto-correlation function (HCACF). A method based on fast Fourier transform (FFT) can be used to calculate the auto-correlation function much faster than the direct method explained below. The numerical implementation of the FFT method is detailed in [26].

In order to better understand what the auto-correlation function is, consider the following example. After a simulation of $(M_t - 1)\Delta t$, the axial heat current is known for t = 0, Δt, $2\Delta t$, ..., $(M_t - 1)\Delta t$. Thus, there are M_t data points available for the calculation of the thermal conductivity. The auto-correlation function at a given time $t = j\Delta t$ (with j = 0, 1, 2, ..., $M_t - 1$) can be calculated using:

$$\mathrm{HCACF}(t) = \frac{1}{M} \sum_{k=1}^{M} j_z(t_k)\, j_z(t_k + t) \tag{2.25}$$

where $M = M_t - j$ and t_1 corresponds to t = 0. Consider a simulation of $10\Delta t$ ($M_t = 11$). The third term (j = 2) of the auto-correlation function can be expressed as:

$$\mathrm{HCACF}(2\Delta t) = \frac{1}{9}\left[j_z(0)\, j_z(2\Delta t) + j_z(\Delta t)\, j_z(3\Delta t) + \ldots + j_z(8\Delta t)\, j_z(10\Delta t) \right] \quad (2.26)$$

Similarly, the fifth term (j = 4) is given by:

$$\mathrm{HCACF}(4\Delta t) = \frac{1}{7}\left[j_z(0)\, j_z(4\Delta t) + j_z(\Delta t)\, j_z(5\Delta t) + \ldots + j_z(6\Delta t)\, j_z(10\Delta t) \right] \quad (2.27)$$

and the last term (j = 10):

$$\mathrm{HCACF}(10\Delta t) = j_z(0)\, j_z(10\Delta t) \quad (2.28)$$

One can notice that the statistical precision of the HCACF is better at early times, since it samples more time origins. It also means that the HCACF at the end of a simulation is not precise and can behave erratically. The integration of the HCACF in Eq. (2.24) is thus limited by the precision of the auto-correlation function, which is influenced by the length of the simulation and by the number of time steps at which the heat current is known.

To overcome this difficulty, it is custom to use a best-fit of the auto-correlation function for times smaller than the time required for phonons to travel ballistically from one end of the nanotube to the other. It might be conservatively estimated as $\tau_b \sim L/c_{LA}$, where $c_{LA} = 20.35\ \mathrm{km/s}$ is the speed of sound of the longitudinal acoustic mode, which is the fast traveling mode in a carbon nanotube [13]. In other words, the best-fit mimics only HCACF($0 < t < \tau_{bf}$), where τ_{bf} is the fitting time. This early time best-fit is required to avoid spurious self-correlation effects that could occur when phonons crossing the PBC interfere with themselves [17]. The most common best-fit is:

$$HCACF_{bf} = A_1 e^{-t/\tau_1} + A_2 e^{-t/\tau_2} \quad (2.29)$$

where A_1, A_2, τ_1, and τ_2 are the parameters to be determined. Physically, τ_1 and τ_2 can be viewed as half the period for energy transfer between two neighboring atoms and as the average phonon-phonon scattering time, respectively [11].

The steps to calculate the thermal conductivity from an EMD simulation are as follow: (1) calculate the heat current auto-correlation function using Eq. (2.25) or the FFT method described in [26] from the heat current data, (2) perform a fitting of the HCACF using Eq. (2.29), (3) calculate the average temperature of the nanotube during the simulation using simulation data, and (4) use the resulting data from steps (1) to (3) in Eq. (2.24) to calculate the thermal conductivity. This post-treatment procedure of EMD simulation results will allow us to study in details the impact of simulation and post-treatment parameters on the calculated thermal conductivity, such as the simulation time (number of time steps) or fitting time.

CHAPTER 3: Sensitivity of MD simulations to post-treatment when determining thermal conductivity of carbon nanotubes

3.1 RÉSUMÉ

Ce chapitre présente les résultats d'un article qui traite d'une étude préliminaire sur l'effet du post-traitement de simulations de dynamique moléculaire à l'équilibre sur le calcul de la conductivité thermique de nanotubes de carbones. L'effet de la durée de la simulation (nombre de pas de temps) sur la reproductibilité des résultats est analysée en calculant la fonction d'auto-corrélation pour des simulations de différentes durées (100,000 à 2,000,000 pas de temps). Les résultats montrent que la durée des simulations que l'on retrouve habituellement dans la littérature pourrait être insuffisante pour minimiser l'impact de la condition initiale du système sur la valeur de la conductivité thermique calculée. On étudie également l'effet de la variation de l'intervalle de temps utilisé lors du calcul de la courbe de tendances de la fonction d'auto-corrélation pour un nanotube d'une longueur de 5 nm.

3.2 INTRODUCTION

Carbon nanotubes have attracted a lot of attention over the last years due to their remarkable properties. In particular, their thermal conductivity has been the subject of various investigations. Depending on the experimental technique and on the nanotube characteristics, thermal conductivity measurements reported in literature present quite a wide range of values, approximately from 300 to 10,000 W/mK [3]-[7]. Such a large range of values has raised some questions regarding the heat transfer properties of carbon nanotubes.

In order to gain a better understanding of the heat transfer behaviour of carbon nanotubes, models have been developed to predict their thermal conductivity. In this work, we focus on molecular dynamics (MD) simulations which calculate the transient evolution of the

position and velocity of each atom of a system, based on Newton's second law. Different types of inter-atomic potentials can be used [21]-[25] to act as the driving forces.

Although conceptually simple, MD simulations proved to be quite challenging. First, they are computationally expensive. Second, examining literature reveals that different authors relying on MD report quite different nanotube thermal conductivities. For example, [27] reported a value of 1,700 W/mK for a 30 nm long (10, 10) nanotube, while [28] reported values ranging from 260 to 400 W/mK for 10 to 400 nm long (10, 10) nanotubes. Both used non-equilibrium molecular dynamics (NEMD) with the same nanotube cross-sectional area. Furthermore, the trends observed are not always the same. Under axial strain, [8] reported that the highest thermal conductivity for a (10, 10) nanotube was obtained when the tube was stretched at 2% of its original length. On the other hand, [9] showed that the optimal thermal conductivity for the same type of nanotube was obtained at 6% compression. Therefore, MD simulations seem relatively sensitive to: (i) the input parameters (e.g., initial velocity distribution, initial temperature of the system, atomic potential, atomic potential parameters, etc.), (ii) the simulation parameters (e.g., length of the simulation, length of the simulation cell, boundary conditions, simulation method, etc.), and (iii) the post-treatment of the simulation results (e.g., number of time steps used to compute the auto-correlation function when using Green-Kubo's formula, number of time steps used for the fitting of the auto-correlation function, number of simulations done while taking averages, etc.).

The objective of the present work is to investigate and document to what extent the post-treatment of the simulation results affects the final value of the thermal conductivity. A brief summary of how MD simulations are performed is first presented. Then, we describe how the length of the simulation (i.e., number of time steps) affects the results. Finally, the influence of the best-fit of the auto-correlation function is reported.

3.3 METHODOLOGY USED FOR MD SIMLUATIONS

In this section, we describe the numerical simulations that have been performed for a 5nm long (10, 10) carbon nanotube using equilibrium molecular dynamics (EMD). The potential used in all simulations is the REBO potential [23], which has been widely used in literature to study carbon nanotubes. The potential parameters used are those already included in the software LAMMPS. Initially, the atoms were located at their equilibrium locations. All atoms were assigned the same velocity vector magnitude, with the average kinetic energy of the system satisfying the equipartition theorem [16]. However, the direction of the velocity vector of each atom was chosen randomly. Then, the velocity of each atom is modified so as to eliminate both the total linear and angular momenta of the system with respect to the center of mass, see [11]. Periodic boundary condition (PBC) is used in the axial direction of the nanotube only.

The time step for all simulations is taken as 0.001 ps. In order to bring the system to an equilibrium state, a NVE (constant number of atoms, volume, and energy) run of 100 ps (i.e. 100,000 time steps) is first done. Then, a 40 ps NVT (constant number of atoms, volume, and temperature) run at T_{MD} = 300 K is done using Nosé-Hoover thermostat. Finally, a NVE run is done for a duration varying from 100 ps to 2,000 ps during which the axial component of the heat current j_z and the system instantaneous temperature are calculated at each time step and written in an output file for post-treatment. Simulations were performed using the open source software LAMMPS on the supercomputer Colosse located at Université Laval (part of CLUMEQ).

The heat current auto-correlation function (HCACF) is calculated using a method based on fast Fourier transform (FFT). The numerical implementation of this method is explained in [26]. The thermal conductivity is related to the heat current auto-correlation function by

$$k = \frac{1}{k_B T^2 L A} \int_0^\infty \langle j_z(0)\, j_z(t) \rangle \, dt \tag{3.1}$$

where k_B is the Boltzmann constant, T is the mean temperature of the system (taken as the average of the instantaneous temperature of the system during the simulation), L and A are the length and cross-sectional area of the nanotube, and j_z is the axial component of the heat current. As explained in [11], there exist many conventions in the literature for the cross-section of a carbon nanotube. The convention used in this work is a ring of van der Waals thickness 0.34 nm. In order to perform the integral in Eq. (3.1), it is custom to use a best-fit of the numerical results for time smaller than the time it takes for a phonon to travel across the nanotube from one end to the other ballistically (τ_b). An estimation method for τ_b is outlined in [11]. The reason to do so is that when using PBC, phonons that leave the simulation cell and re-enter can interfere with themselves, causing an artificial correlation [17]. However, not all authors use fitting times smaller than τ_b. The most common best-fit is

$$HCACF_{bf} = A_1 e^{-t/\tau_1} + A_2 e^{-t/\tau_2} \tag{3.2}$$

where A_1, A_2, τ_1, and τ_2 are the parameters to be determined. The best-fit of the auto-correlation function can then be integrated and used in conjunction with Eq. (3.1) to obtain the thermal conductivity of the carbon nanotube.

3.4 EFFECT OF THE SIMULATION TIME

The first numerical experiment consisted in varying the duration of the MD simulation. In literature, the total duration of MD simulations for a similar tube is typically between 400 and 1,000 ps. In the present experience, simulations were performed over a total number of 2,000,000 time steps (i.e. 2,000 ps). Then, the auto-correlation function was calculated starting from the first time-step up to a certain number of time steps (between 100,000 and 2,000,000). The procedure was repeated five times with different initial distributions of velocity. The resulting thermal conductivities are shown in Fig. 3.1 as a function of the number of time steps used to calculate the heat current auto-correlation function. The fitting time used to calculate the thermal conductivity for all five simulations in Fig. 3.1

is $\tau_{bf} = 10\tau_b$. Fig. 3.1(a) presents the result of the individual five runs while Fig. 3.1(b) reports the average and standard deviation of k (error bars based on the 5 runs).

For a given run, one can observe that the thermal conductivity can vary significantly with the simulation time, especially when the simulation time is below 500,000 time steps. For example, considering the pink series of points in Fig. 3.1(a), k varies from 240 W/mK based on a simulation of 100,000 time steps, to 425 W/mK based on a simulation of 500,000 time steps. Furthermore, for such simulation lengths, a variation in the initial velocity distribution can cause large variations in the thermal conductivity. This explains the large standard deviations in Fig. 3.1(b) for simulations of less than 500,000 time steps. Based on Fig. 3.1, it would be hazardous to use simulations of less than 500,000 time steps as the dispersion of the results is quite large.

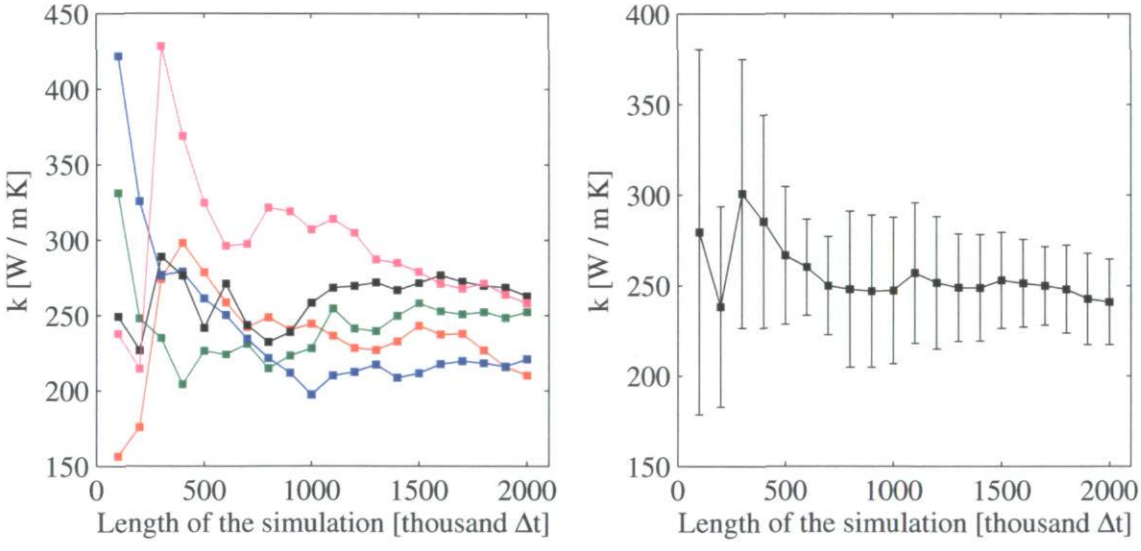

a) b)

Figure 3.1: Effect of the length of the simulation on the thermal conductivity value; a) for 5 different runs, and b) average and standard deviation.

3.5 EFFECT OF THE FITTING TIME

Since the auto-correlation function is typically unsmooth, because the uncertainty on the auto-correlation function increases with time (the number of different time origins sampled decreases when time increases), and most importantly, since there exist spurious self-correlation effects when using PBC, most authors use a best-fit to analyze the results of a MD simulation, see Eq. (3.2). Four best-fit parameters are to be determined by minimizing the error between the simulation results and the fitting. However, the time frame over which to perform the fitting of the auto-correlation function (τ_{bf}) is different among authors. For example, [11] used $\tau_{bf} < \tau_b$ and obtained a value of k ~ 30 W/mK, while [29] used $\tau_{bf} = 12\tau_b$ and reported a value of k ~ 1,600 W/mK for a similar nanotube. For the nanotube considered here, the value of τ_b is approximately 0.25 ps.

We analyzed the results of the simulations presented above by determining the best-fit, Eq. (3.2), based on different time frames τ_{bf} (i.e., number of τ_b intervals). In other words, only the auto-correlation function datasets for t smaller than the time frame considered were used to determine the best-fit. The results are shown in Fig. 3.2(a) for 5 different runs, and the average and standard deviation is reported in Fig. 3.2(b) (excluding values in the non-converging time interval). Important variations of k are found depending on the number of τ_b intervals used to find the best-fit. The thermal conductivity found is ~ 30 W/mK when very small fitting times are used. This result is in good agreement with the value reported by [11]. However, for such small fitting times, the best-fit only considers time steps that are part of the fast initial decay of the auto-correlation function, likely underestimating the thermal conductivity. If the fitting time is made larger but is still under τ_b, there is a non-convergence effect in the thermal conductivity value. This effect occurs because the auto-correlation function has a peak in this time interval, see Fig. 3.3. This causes the best-fit to greatly overestimate the long decay time of the auto-correlation function, resulting in a very large, unphysical value for the thermal conductivity, which is why no points are reported in Fig. 3.2 for that interval of τ_{bf}. If a fitting time larger than τ_b is used, the thermal conductivity converges towards a value larger than the one found

for very small fitting times (average of 210 W/mK for $\tau_{bf} = 2\tau_b$). As τ_{bf} continues to increase, the value of k also increases up to an average of 275 W/mK when $\tau_{bf} = 20\tau_b$.

In order to illustrate how τ_{bf} influences the resulting conductivity, we show in Fig. 3.3 an example of auto-correlation function as a function of t compared to two best-fits. In Fig. 3.3(a), the best-fit was determined on $\tau_{bf} = \tau_b$, while in Fig. 3.3(b) it was determined on $\tau_{bf} = 20\tau_b$. When using $\tau_{bf} = \tau_b$, the fitting doesn't represent properly the slow exponential decay behaviour of the HCACF at later times (that may well result from spurious self-correlation effects). It is also possible to see that for this fitting time (t < 0.25 ps), the auto-correlation function has a peak which makes the best-fit to decay more slowly, giving a higher thermal conductivity value. This effect is even more pronounced for fitting times smaller than τ_b. However, if one is using a longer fitting time, for example $20\tau_b$, the fitting will represent this long exponential decay better, and yield values that will slowly converge. Fitting times longer than $20\tau_b$ have also been studied. Another increasing jump in the thermal conductivity might occur if the fitting time is further increased, when the fast initial exponential decay is no longer taken into account by the best-fit. This results in a better fitting of the slow, exponential decay and higher thermal conductivity values.

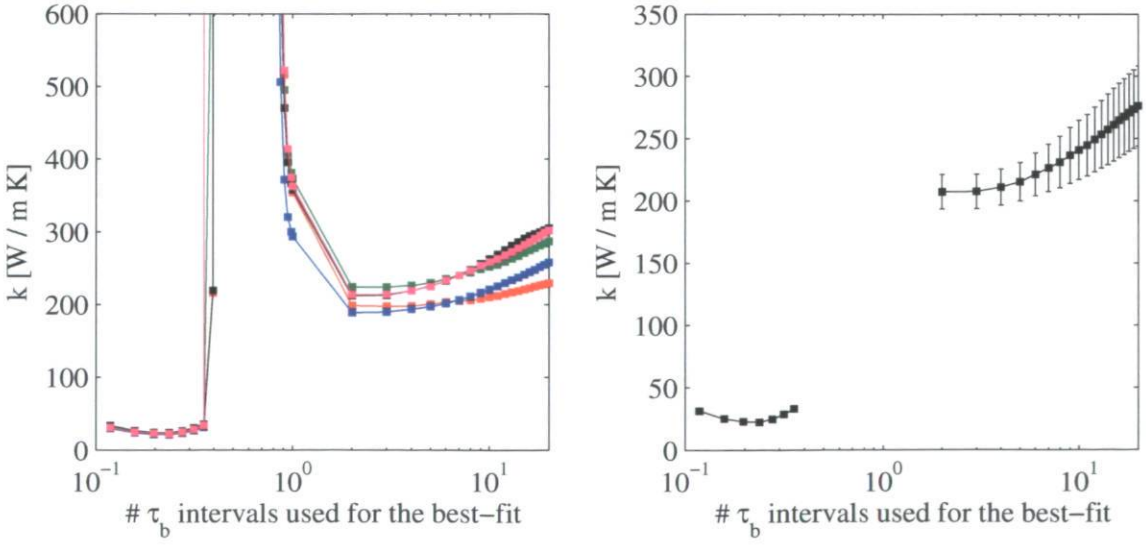

Figure 3.2: Effect of τ_{bf} (number of τ_b intervals) for the best-fit;
a) for 5 different runs, and b) average and standard deviation.

Those results might partially explain why different values can be found in the literature for different fitting times. As pointed out earlier, [11] reported a value of k ~ 30 W/mK while using a fitting time smaller than τ_b. This low value may be caused by the best-fit only sampling times that are part of the initial fast decay of the auto-correlation function. On the other hand, [29] reported a value of k ~ 1,600 W/mK using a fitting time greater than τ_b. This may be explained by the best-fit that better represents the long and slow exponential decay of the auto-correlation function. However, it is known that for such times, there may be some artificial correlation effects. Furthermore, they used a simulation time of 400 ps, which has been shown to be insufficient to minimize the error occurring from different initial velocity distributions. Combined with the large fitting time used by the authors, this might explain why they obtained such high thermal conductivity values.

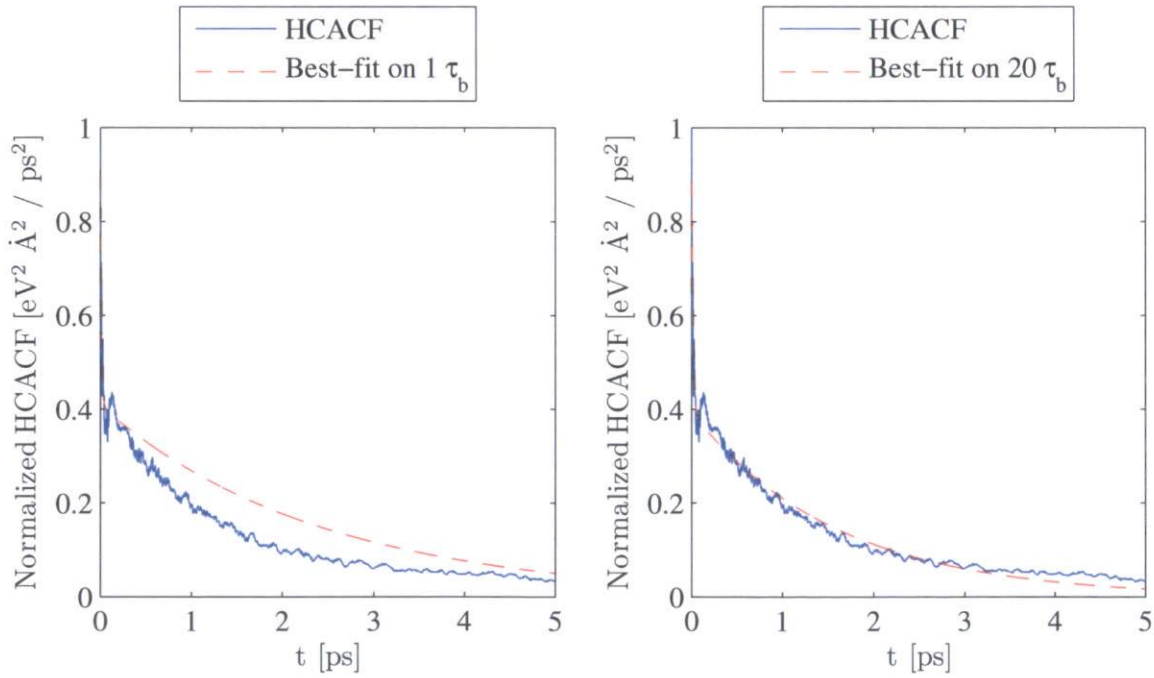

Figure 3.3: Examples of auto-correlation functions and best-fits;
a) Best-fit with $\tau_{bf} = 1\tau_b$, and b) Best-fit with $\tau_{bf} = 20\tau_b$.

3.6 CONCLUSIONS

In the present work, the effect of post-treatment has been studied for the calculation of the thermal conductivity of a 5 nm long (10, 10) carbon nanotube using Green-Kubo relation. It has been shown that the number of time steps usually used for MD simulations in the literature might not be sufficient to ensure that a difference in the initial condition of the system has fewer repercussions on the resulting thermal conductivity. Moreover, the time interval used for the fitting of the auto-correlation function has been studied over a wide interval. For a 5 nm long nanotube, it is difficult to recommend any fitting time because of the small time taken by phonons to traverse ballistically the nanotube. If too small fitting times are used, only the fast initial decay of the auto-correlation function is fitted, resulting in an underestimation of the thermal conductivity. If too large fitting times are used, the portion of the auto-correlation function that might be the result of an artificial correlation is fitted. This behaviour of the thermal conductivity as a function of the fitting time may be different, however, for longer carbon nanotubes, since their τ_b is larger and the shape of the auto-correlation function should not vary significantly. The study of the effect of post-treatment for larger nanotubes shall be the subject of future studies.

CHAPTER 4: Impact of the post-treatment of equilibrium molecular dynamics (EMD) simulations when determining the lattice thermal conductivity of carbon nanotubes

4.1 RÉSUMÉ

Ce chapitre contient les résultats d'un article visant à poursuivre l'étude présentée lors du précédent chapitre. On analyse en détails l'impact du post-traitement de simulations de dynamique moléculaire à l'équilibre sur la conductivité thermique pour des nanotubes de différentes longueurs. On propose une méthode pour déterminer la durée minimale d'une simulation reposant sur l'impact de la condition initiale sur la conductivité thermique calculée. Une étude systématique sur l'impact du choix de l'intervalle de temps utilisé pour le calcul de la courbe de tendances de la fonction d'auto-corrélation pour des nanotubes de différentes longueurs est ensuite présentée. À la lumière des résultats, il est suggéré que l'effet de longueur rencontré dans la littérature pourrait être attribué en partie au choix de cet intervalle de temps. On observe également qu'il est possible d'obtenir la même conductivité thermique pour des nanotubes de différentes longueurs en choisissant un intervalle de temps suffisamment long.

4.2 INTRODUCTION

After the discovery of carbon nanotubes (CNTs), Sumio Iijima has published a paper [1] that has generated an increased interest in those molecules which have both remarkable electrical and thermal properties. For instance, some investigations on carbon nanotubes have reported a very high thermal conductivity [2]. Depending on the experimental technique, operating conditions, and on the nanotube characteristics, thermal conductivity measurements reported in literature vary approximately from 300 to 10,000 W/m K [3-7].

The experimental measurement of the thermal conductivity of an isolated CNT can prove to be very difficult [3]. Furthermore, the chirality of the studied CNT, which influences its thermal conductivity, is hardly known. Because of this, numerical models have been developed to gain a better understanding of the heat transfer mechanisms in carbon nanotubes. Molecular Dynamics (MD) simulation is a numerical tool that can be used to study the thermal properties of CNTs with a given chirality. It consists in determining the transient evolution of the position and velocity of a system of particles by solving Newton's second law. There are typically two main methods for determining the thermal conductivity of carbon nanotubes using MD simulations: equilibrium molecular dynamics (EMD) and non-equilibrium molecular dynamics (NEMD). EMD simulations [30] consist in the calculation of the position and the velocity of each atom in an equilibrium system. From this data, the instantaneous heat flux can be computed and used to estimate the thermal conductivity. NEMD simulations [31] differ from EMD simulations in that the system simulated is not in an equilibrium state. A thermal gradient is introduced in the system by adding a hot and a cold reservoir at each end of the carbon nanotube. Those reservoirs are kept at constant temperature by adding energy in the hot reservoir and removing energy in the cold reservoir at each time step. Once the system has reached a steady-state, the temperature profile in the carbon nanotube is calculated and the thermal conductivity is obtained from Fourier's law of conduction. Note that there are other methods that differ from EMD simulations performed in this work that can be used to predict the phonon properties in a carbon nanotube and then estimate the thermal conductivity, such as the Boltzmann transport equation lattice dynamics (BTE-LD) method [32], the Boltzmann transport equation molecular dynamics (BTE-MD) method [32], or the spectral energy density method [33]. However, those methods do not use the integration of the heat current auto-correlation function to estimate the thermal conductivity, so they will not be addressed in the present work.

Presently, there is no agreement in literature on the exact value of the thermal conductivity of carbon nanotubes [11]. Moreover, the trends observed can be very different. For example, the effect of the application of external mechanical strain on a carbon nanotube on its thermal conductivity has already been addressed in the past [8,9],

but the reported results are contradictory. The maximal thermal conductivity reported by Ren et al. [8] for a (10, 10) CNT under axial strain was obtained when the CNT was stretched at 2% of its original length. On the opposite, Li et al. [9] reported that the maximal thermal conductivity value for a (10, 10) CNT was obtained when the CNT was compressed at 6% of its original length. The explanation of discrepancies found in literature about the numerical calculation of the thermal conductivity of CNTs using MD simulations is still an open topic [10,11].

The present work addresses the post-treatment of the results of equilibrium molecular dynamics simulations when determining the thermal conductivity of carbon nanotubes. It is important to emphasize that the focus of this work is not on determining the exact value of the thermal conductivity of a carbon nanotube, but rather on the equilibrium molecular dynamics post-treatment approach, and in particular the use of a best-fit of the heat current auto-correlation function. If the results from different simulations are to be compared, then the methods used and their shortcomings must first be clearly understood. The purpose of this work is thus to study in details the EMD method with a best-fit of the auto-correlation function, and to explain some of the differences in the calculated thermal conductivity found in literature. In the first section, the numerical procedure of the MD simulations is detailed. Then, a study of the thermal conductivity as a function of the simulation time is presented. A method to determine the required simulation time (i.e., number of time steps) that minimizes the impact of the initial condition on the thermal conductivity is introduced. In the next two sections, a thorough analysis of the thermal conductivity as a function of the fitting time when using a double-exponential best-fit of the auto-correlation function is presented. The main behaviors of the best-fit and the shortcomings of this method are addressed. The thermal conductivity as a function of the fitting time for different nanotube lengths is also studied. In the last section, a comparison between simple and double-exponential best-fits is presented.

4.3 NUMERICAL PROCEDURE

In this section, we summarize briefly how the molecular dynamics simulations were performed and post-treated in order to estimate the thermal conductivity of carbon nanotubes. Given a nanotube length and chirality, the atoms were initially positioned at the equilibrium position with a bond length of 1.42 Å. A velocity vector with random direction in space was assigned to each atom, sampled from a uniform velocity distribution at the temperature considered. The velocity of all atoms was then modified in order to eliminate the total momentum (linear and angular) of the system using the following mathematical procedure [11]:

$$\vec{v}_{i,new} = \vec{v}_{i,old} - \frac{1}{N}\sum_{j=1}^{N} \vec{v}_{j,old} - \vec{\omega} \times \vec{r}_i \tag{4.1}$$

where $\vec{v}_i$ and $\vec{r}_i$ denote the velocity and position vector of the i^{th} atom, N is the total number of atoms, and $\vec{\omega}$ is the angular velocity of the system. The details of the calculation of the angular velocity of the system are given in Goldstein [18]. In the present work, the chirality of all nanotubes is (10, 10) and the initial temperature of the system is 300 K for all simulations.

Before running a simulation, the initial setting (i.e. the initial position, velocity, and mass of the atoms) was imported in the LAMMPS [14,15] software. The potential used for all simulations is the REBO potential [23] with the default parameters for carbon atoms included in LAMMPS. Periodic boundary conditions (PBC) were considered in the axial direction of the nanotube. The simulations were carried out in three steps: first, an equilibration NVE run (with constant number of atom N, volume V, and energy E) is performed for 100 ps in order to allow the system to reach equilibrium, i.e. to achieve a Maxwell-Boltzmann velocity distribution. Second, an NVT run (with constant number of atom N, volume V, and temperature T) is performed for 400 ps to bring the system to the desired temperature. During these two steps, the temperature, total momentum, center of mass position, and center of mass velocity of the system are monitored. The 400 ps NVT

run is found to be sufficiently long to allow the system to reach the desired temperature. The zero total momentum, position, and velocity of the system are well preserved during the equilibration process. Moreover, the resulting velocity distribution is in agreement with the Maxwell-Boltzmann distribution. After the equilibration runs, an NVE run is performed for 2,000 ps during which the heat current and the mean temperature of the system are calculated at each time step using the LAMMPS compute heat/flux and compute temp commands and stored in output files. The time step is 1 fs for all simulations.

The output data is used to calculate the lattice thermal conductivity of the carbon nanotube using the following equation, which can be derived from the linear response theory [16]:

$$k = \frac{1}{k_B T^2 LA} \int_0^\infty \langle j_z(0) j_z(t) \rangle dt \tag{4.2}$$

where k_B is the Boltzmann constant, T is the temperature of the system (taken as the average of the mean temperature of the system during the simulation), L and A are the length and cross-sectional area of the nanotube, and j_z is the axial component of the heat current. There are different conventions for the cross-sectional area of a nanotube [11], but the one used in all simulations of the present work is a ring with a thickness equal to 3.4 Å. In Eq. (4.2), $\langle j_z(0) j_z(t) \rangle$ is called the heat current auto-correlation function (HCACF). A method based on fast Fourier transform (FFT) is used to calculate the auto-correlation function much faster than the direct method explained below. The numerical implementation of the FFT method is explained by Allen and Tildesley [26].

In order to better understand what the auto-correlation function represents, consider the following example. After a simulation of $(M_t - 1)\Delta t$, the axial heat current is known for t = 0, Δt, $2\Delta t$, …, $(M_t - 1)\Delta t$. Thus, there are M_t data points available for the calculation of the thermal conductivity. The auto-correlation function at a given time $t = j\Delta t$ (with j = 0, 1, 2, …, $M_t - 1$) can be calculated using:

$$\mathrm{HCACF}(t) = \langle j_z(0) j_z(t) \rangle = \frac{1}{M} \sum_{k=1}^{M} j_z(t_k) j_z(t_k + t) \tag{4.3}$$

where $M = M_t - j$ and t1 corresponds to t = 0. For the sake of illustration, consider a simulation of $10\Delta t$ (i.e., Mt = 11). Then, for example, the third term (j = 2) of the auto-correlation function can be expressed as:

$$\mathrm{HCACF}(2\Delta t) = \frac{1}{9}\left[j_z(0) j_z(2\Delta t) + j_z(\Delta t) j_z(3\Delta t) + \ldots + j_z(8\Delta t) j_z(10\Delta t) \right] \tag{4.4}$$

Similarly, the fifth term (j = 4) is given by:

$$\mathrm{HCACF}(4\Delta t) = \frac{1}{7}\left[j_z(0) j_z(4\Delta t) + j_z(\Delta t) j_z(5\Delta t) + \ldots + j_z(6\Delta t) j_z(10\Delta t) \right] \tag{4.5}$$

and the last term (j = 10):

$$\mathrm{HCACF}(10\Delta t) = j_z(0) j_z(10\Delta t) \tag{4.6}$$

One can notice that the statistical precision of the HCACF is better at early times, since it samples more time origins. It also means that the HCACF for large time is not precise and can behave erratically. The integration of the HCACF in Eq. (4.2) is thus limited by the precision of the auto-correlation function, which is influenced by simulation time and by the number of time steps at which the heat current is known.

It has been suggested by some authors to perform a best-fit of the auto-correlation at early times to avoid spurious self-correlation effects [11,17]. In other words, the best-fit mimics only HCACF($0 < t < \tau_{bf}$), where τ_{bf} is the fitting time. It is worth to mention that HCACF(t) involves combination of heat currents evaluated at all the discrete times of the simulation (even times larger than t), see Eqs. (4.5) or (4.6). The fitting time τ_{bf} is

chosen in regards to τ_b, the time required for a phonon to travel ballistically from one end of the nanotube to the other. It might be conservatively estimated as $\tau_b \sim L/c_{LA}$, where $c_{LA} = 20.35\ km/s$ is the speed of sound of the longitudinal acoustic mode, which is the fast traveling mode in a carbon nanotube [13]. For lengths of approximately 5, 10, 20, 40, 200, and 1000 nm, the ballistic times τ_b are thus 0.242, 0.484, 0.968, 1.936, 9.680, and 48.400 ps, respectively. The most common best-fit is:

$$HCACF_{bf} = A_1 \exp(-t/\tau_1) + A_2 \exp(-t/\tau_2) \tag{4.7}$$

where A_1, A_2, τ_1, and τ_2 are the parameters to be determined. Physically, τ_1 and τ_2 can be viewed as half the period for energy transfer between two neighboring atoms and as the average phonon-phonon scattering time, respectively [11]. The best-fit of the auto-correlation function, Eq. (4.7), can be used in Eq. (4.2) to calculate the thermal conductivity. The impact of the time τ_{bf} used for the best-fit of the HCACF, which is a post-treatment parameter, will be studied in later sections.

4.4 SIMULATION TIME

The simulation time (i.e., number of time steps) is an important factor when calculating the thermal conductivity using equilibrium molecular dynamics, since it will determine the amount of heat current data available for the calculation of the HCACF. As explained in the previous section, if the simulation is not long enough, the statistical precision of the HCACF will be poor and the calculated thermal conductivity could be erroneous. On the other hand, if the simulation is too long, it will be computationally expansive and it will require a lot of memory to store all the simulation results. The post-treatment of such a large amount of data can be tedious and can further increase the computational time of a simulation. However, literature does not propose a formal method to determine the required simulation time when calculating the thermal conductivity. A common simulation time for simulations similar to those reported in the present work is a 40 ps NVT run followed by a 400 ps NVE run [11,29,34]. Some authors, however, have used

much larger simulation times. In their work, Donadio and Galli [35] used a 200 ps NVT run followed by a 8 ns NVE run. In this section, a method based on the impact of the initial condition on the calculated thermal conductivity is proposed to determine the minimal simulation time.

Because of the statistical nature of atomistic systems, a slight variation in the initial condition (e.g., a different orientation of the initial velocity vectors) will give different atom trajectories during the simulation, different heat currents, and thus can result in different thermal conductivities. Using the aforementioned numerical procedure for (10, 10) CNTs of different lengths, the lattice thermal conductivity has been calculated as a function of the simulation time, τ_s. The studied nanotubes are made of 800, 1600, 3200, 6400, 32000, and 160000 atoms, with respective lengths of approximately 5, 10, 20, 40, 200, and 1000 nm. For each length, 5 independent initial conditions have been tested. It is important to emphasize that only one simulation is performed for each initial condition. The time used for the best-fit in all cases is equal to τ_b, i.e. the best-fit of the HCACF is calculated using data points of HCACF from t = 0 to t = τ_b in each case. The simulation time studied in the present work varies from 100 ps to 2,000 ps at intervals of 100 ps, i.e. τ_s = 100, 200, ..., 1,900, and 2,000 ps. The thermal conductivity as a function of the simulation time for L = 5 nm and L = 200 nm is shown in Fig. 4.1(a) and (c), respectively. Each series of points represents one initial condition. The mean thermal conductivity and standard error (from the 5 different initial conditions) are shown in Fig. 4.1(b) and (d) for the same lengths (5 nm and 200 nm, respectively). It can be seen that the impact of the initial condition on the thermal conductivity is significant for simulation time under 500 ps for both lengths. The mean thermal conductivity "converges" for simulation times exceeding approximately 1,500 ps, where the standard error is the smallest. This procedure was repeated for all lengths mentioned above, and this trend was observed for carbon nanotubes of all lengths. Many authors [11,29,34] use a simulation time of 400 ps for simulations similar to those reported here, which might result in a significant impact of the initial condition on the calculated thermal conductivity, according to Fig. 4.1. It also means that the HCACF (and thus the thermal conductivity)

will be calculated with less statistical precision, since there are less heat flux data points available when using smaller simulation times. For these reasons, the simulation time is taken as 2,000 ps for the rest of this work.

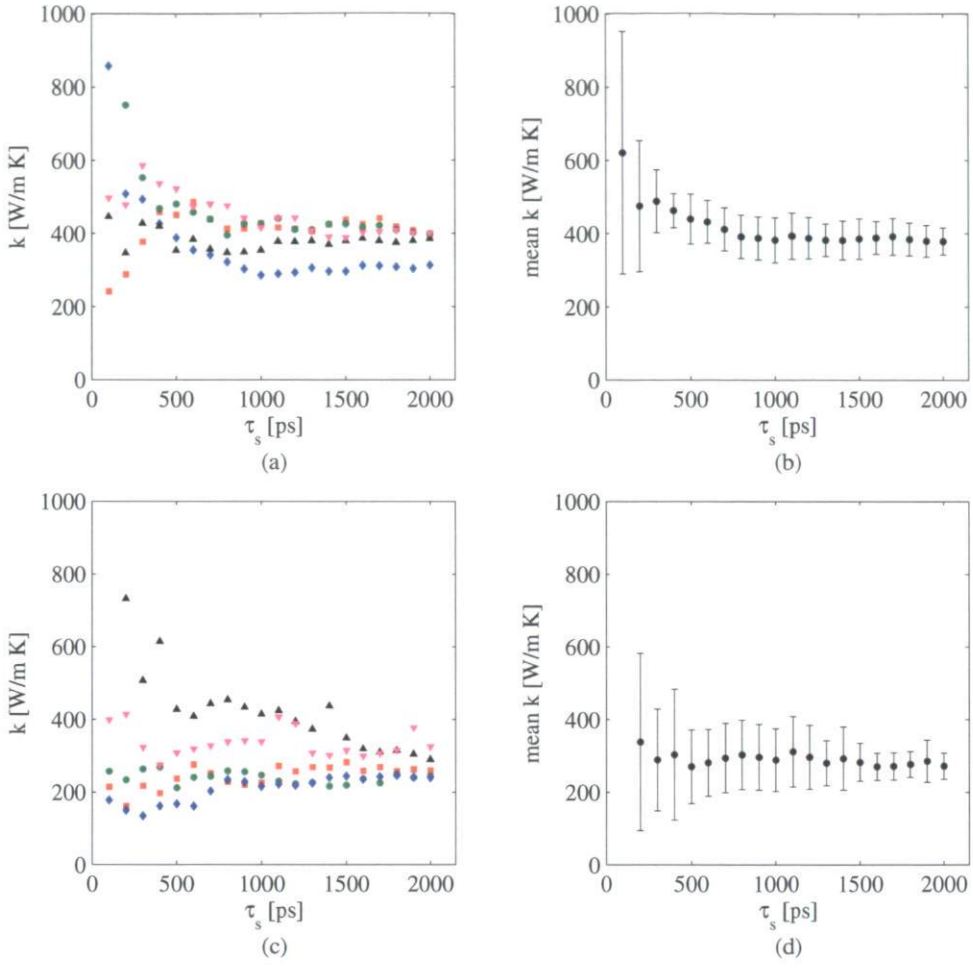

Figure 4.1: Thermal conductivity as a function of the simulation time τ_s with $\tau_{bf} = \tau_b$ for: (a) L = 5 nm with 5 different initial conditions, (b) mean thermal conductivity and standard error for L = 5 nm, (c) L = 200 nm with 5 different initial conditions, and (d) mean thermal conductivity and standard error for L = 200 nm

4.5 FITTING TIME: NON-UNIQUENESS OF SOLUTIONS

As explained previously, it has been suggested to use fitting times smaller than τ_b in order to avoid spurious self-correlation effects [11,17]. Those effects arise when using PBCs because phonons that leave the simulation domain at one end and reenter at the other end might interfere with themselves. However, not all authors use fitting times smaller than τ_b [29]. The impact of the fitting time τ_{bf} on the calculated thermal conductivity has yet to be addressed. In this section, the impact of the choice of the fitting parameter τ_{bf} is studied in details for different carbon nanotube lengths and initial conditions (the same simulations as in the previous section are used). Values of τ_{bf} smaller and larger than τ_b are considered. In order to minimize the impact of the initial condition, the simulation time is 2,000 ps in all cases. For all lengths except 1000 nm, the value of the fitting time studied varies from 0.01 ps (10 time steps) to τ_b with intervals of 0.01 ps when $\tau_{bf} < \tau_b$, and from τ_b to $20\tau_b$ with intervals of τ_b for $\tau_{bf} \geq \tau_b$. For the 1000 nm long nanotube, the value of the fitting time varies from 0.02 ps (20 time steps) to τ_b with intervals of 0.02 ps when $\tau_{bf} < \tau_b$. The best-fit of the auto-correlation function is performed with the least-square method in conjunction with the Nelder-Mead simplex optimization algorithm as described in Lagarias et al. [36]. A preliminary study of the dependence of the thermal conductivity with the fitting time has been presented in the previous chapter.

The thermal conductivity as a function of τ_{bf}, $k(\tau_{bf})$, is presented for five different simulations for a 200 nm long CNT in Fig. 4.2. Each curve represents a different initial condition (different orientation of the velocity vectors) at the same temperature. An important feature of $k(\tau_{bf})$ that can be noticed in this figure is the non-uniqueness of the solution of the best-fit for fitting times approximately smaller than 10 ps. There are two main solutions leading to very different behaviors of the thermal conductivity as a function of τ_{bf}. The first main behavior (lower branch in Fig. 4.2) is an increase of the thermal conductivity with the fitting time from k ~ 25 W/m K to a "converged" value of k

~ 300 W/m K for $\tau_{bf} \gtrsim \tau_b$. The other main behavior (upper branch in Fig. 4.2) is a decrease of the thermal conductivity followed by an increase as the fitting time increases. There are other possible solutions to the best-fit depending on the fitting time used, as can be seen from the other points in Fig. 4.2 for $\tau_{bf} < \tau_b$. The initial guess of the fitting parameters will also influence the solution towards which the best-fit of the HCACF will converge. An example of this phenomenon is illustrated in Fig. 4.3 for a 40 nm long CNT. The initial guess of the fitting parameters in Fig. 4.3(a) are A_1 = 6,000 $(eV\text{Å}/ps)^2$, A_2 = 5,000 $(eV\text{Å}/ps)^2$, τ_1 = 0.01 ps, and τ_2 = 1 ps, as compared to A_1 = 16,000 $(eV\text{Å}/ps)^2$, A_2 = 5,000 $(eV\text{Å}/ps)^2$, τ_1 = 0 ps, and τ_2 = 10 ps in Fig. 4.3(b). The optimized fitting parameters are $A_1 \approx$ 49,200 $(eV\text{Å}/ps)^2$, $A_2 \approx$ 45,000 $(eV\text{Å}/ps)^2$, $\tau_1 \approx$ 0.0109 ps, and $\tau_2 \approx$ 1.3338 ps in Fig. 4.3(a) and $A_1 \approx$ 50,400 $(eV\text{Å}/ps)^2$, $A^2 \approx$ 37,900 $(eV\text{Å}/ps)^2$, $\tau_1 \approx$ 0.0182 ps, and $\tau_2 \approx$ –78.1580 ps in Fig. 4.3(b). If one observes Fig. 4.3 closely, both best-fits behave correctly over the fitting time period of 0.4 ps. However, the negative sign before τ_2 in the second case means that the integral of the best-fit in Eq. (4.2) will diverge, and thus no finite value of thermal conductivity can be obtained from those parameters. This is an extreme example just to illustrate how the initial guess of the fitting parameter can influence the calculated thermal conductivity. When performing the best-fit of the auto-correlation function, τ_1 and τ_2 should always be positive.

Even though the solution of the best-fit of the auto-correlation function is not unique, the thermal conductivity of a CNT should be. Therefore, there must be only one physically correct solution. In order to understand the difference between each solution, the normalized HCACFs and their corresponding best-fits are presented in Fig. 4.4 for two specific cases. In Fig. 4.4(a), the fitting time used is 0.54 ps (540 time steps) while in Fig. 4.4(b), it is 0.55 ps (550 time steps). In the first case, the double-exponential behavior of the HCACF is well represented. The calculated thermal conductivity for this fitting time is 210 W/m K, which corresponds to the upper branch of $k(\tau_{bf})$ in Fig. 4.2. In the second case, however, the fast initial decay of the HCACF is not well captured. The best-fit of the HCACF shows a single-exponential behavior. The thermal conductivity in that case is 170 W/m K, which corresponds to the lower branch of $k(\tau_{bf})$.

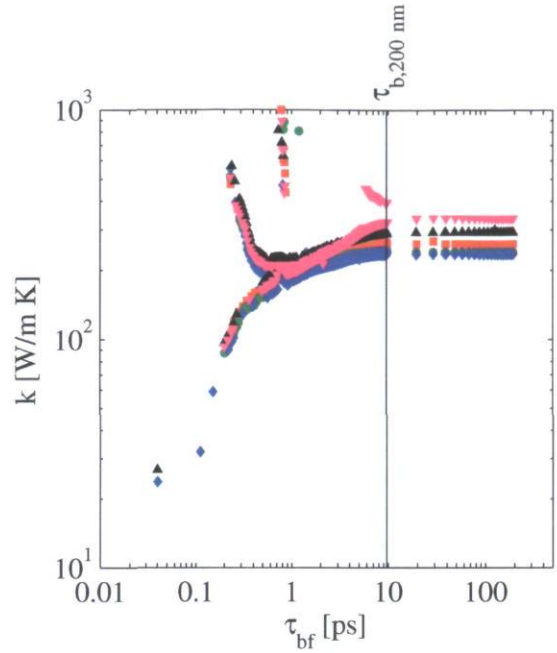

Figure 4.2: Thermal conductivity as a function of the fitting time τ_{bf} with τ_s = 2,000 ps for L = 200 nm with 5 different initial conditions

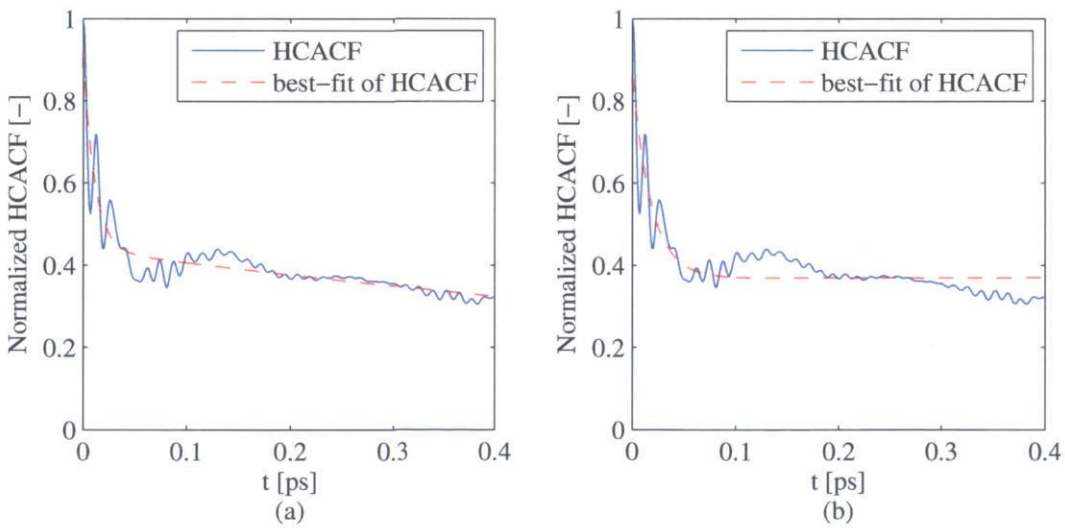

Figure 4.3: Influence of the initial guess of the fitting parameters on the best-fit of the auto-correlation function

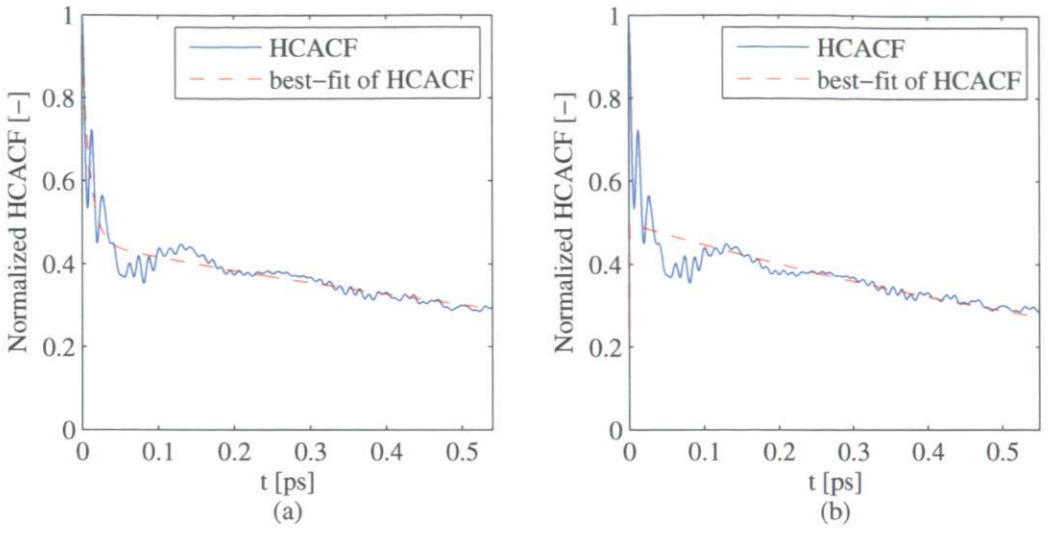

Figure 4.4: Existence of two possible solutions for the best-fit: (a) double-exponential behavior, and (b) single-exponential behavior

There is another very important behavior of $k(\tau_{bf})$ that is not shown in Fig. 4.4. If the fitting time is larger than the period of the fast initial decay of the HCACF but is small enough not to include a significant portion of the slow exponential decay, the thermal conductivity might diverge. This is due to the transition between fast and slow exponential decays of the HCACF. The best-fit of the HCACF for a 5 nm long CNT with a 0.2 ps (200 time steps) fitting time is shown in Fig. 4.5. The decay time of the slow exponential decay in this case is very large. Since the thermal conductivity is related to the integral of the HCACF when using the Green-Kubo formalism, then the calculated thermal conductivity in that case will be several orders of magnitude above any physically plausible value. The fitting time of 0.2 ps is smaller, but very close to the ballistic time for a 5 nm long CNT, which is 0.242 ps. This means that for such small nanotubes, using fitting times smaller than τ_b will either result in a fitting of the fast initial decay of the HCACF only (which is not the largest contribution to the thermal conductivity) or in non-physical thermal conductivities. The use of $\tau_{bf} > \tau_b$ is necessary in that case if one wants to include the slow exponential decay in the best-fit. For the 5

nm long CNT, the use of fitting times smaller than the ballistic times resulted in thermal conductivity values of the order of 25 W/m K, which is very similar to the values reported by Lukes and Zhong [11] for nanotubes of the same length. This value, however, only takes into account the fast initial decay of the HCACF. A similar behavior of k vs τ_{bf} is obtained for other tested lengths.

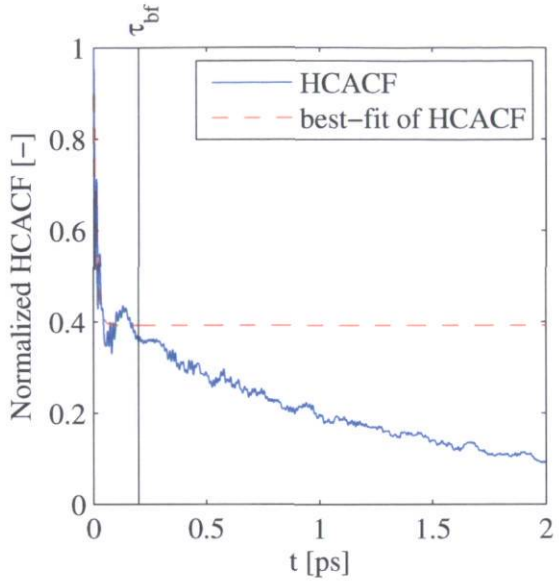

Figure 4.5: Divergence of the thermal conductivity when using small τ_{bf}

4.6 FITTING TIME: EFFECT OF THE NANOTUBE LENGTH

The effect of the length of the nanotube on the calculated thermal conductivity when using PBC in the axial direction has been studied in the past by many authors [11,29,34]. Similar observations have been reported, i.e. an increase in thermal conductivity which eventually converges towards a certain value as the length of the carbon nanotube increases (length effect). The thermal conductivity as a function of both the fitting time and the length of the nanotube is shown in Fig. 4.6(a) for each studied length. For more clarity, only one simulation is shown per length. A zoom of the central part of this figure is also presented in Fig. 4.6(b). As was previously mentioned, the same behavior can be observed for all lengths. The most interesting feature is that not only does $k(\tau_{bf})$

behaves similarly, but the thermal conductivity as a function of the fitting time is roughly the same for all lengths. Since the thermal conductivity reaches a "converged" value for large fitting times, it would be logical to use nanotube length that allows to calculate this converged thermal conductivity while still respecting the constraint $\tau_{bf} < \tau_b$. That means that a length of at least 200 nm would be necessary to calculate the lattice thermal conductivity of a carbon nanotube using EMD simulations with PBCs. However, as the same result could be obtained when using shorter CNTs and fitting times larger than τ_b, the necessity to use fitting times τ_{bf} smaller than the ballistic time τ_b could be questioned.

Another interesting observation is that the "length effect" on the calculated thermal conductivity reported in literature could possibly be – at least in part – an effect of the fitting time when using $\tau_{bf} < \tau_b$. Since τ_b increases with length, so would the thermal conductivity until it reaches a converged value according to Fig. 4.6. That behavior would still occur if the thermal conductivity would be an average of values from the lower and upper branches in Fig. 4.6. For example, the thermal conductivity as a function of length presented by Lukes and Zhong [11] is very similar to the lower branch of $k(\tau_{bf})$ in Fig. 4.6(a). In their work, a fitting time smaller than τ_b has been used for all lengths (the exact value of the fitting time was not mentionned). Grujicic et al. [29] also present a curve with a similar trend for the thermal conductivity as a function of length, although the thermal conductivity is approximately one order of magnitude higher than the one in the present work. In their work, a fitting time of 3 ps is used regardless of the length of the nanotube. In Fig. 6(a), a fitting time of 3 ps corresponds to the convergence zone of the thermal conductivity, where similar results are obtained for all lengths. Considering the large error bars reported in their work (based on five simulations with different initial conditions), it is difficult to attribute an unambiguous length effect on the thermal conductivity (i.e., error bars for the thermal conductivity of CNTs of different lengths overlap). The same observation could be made for the results presented by Che et al. [34] who also used a fitting time of 3 ps. In their work, the standard errors are even larger, and there is also an overlap of the error bars for all lengths.

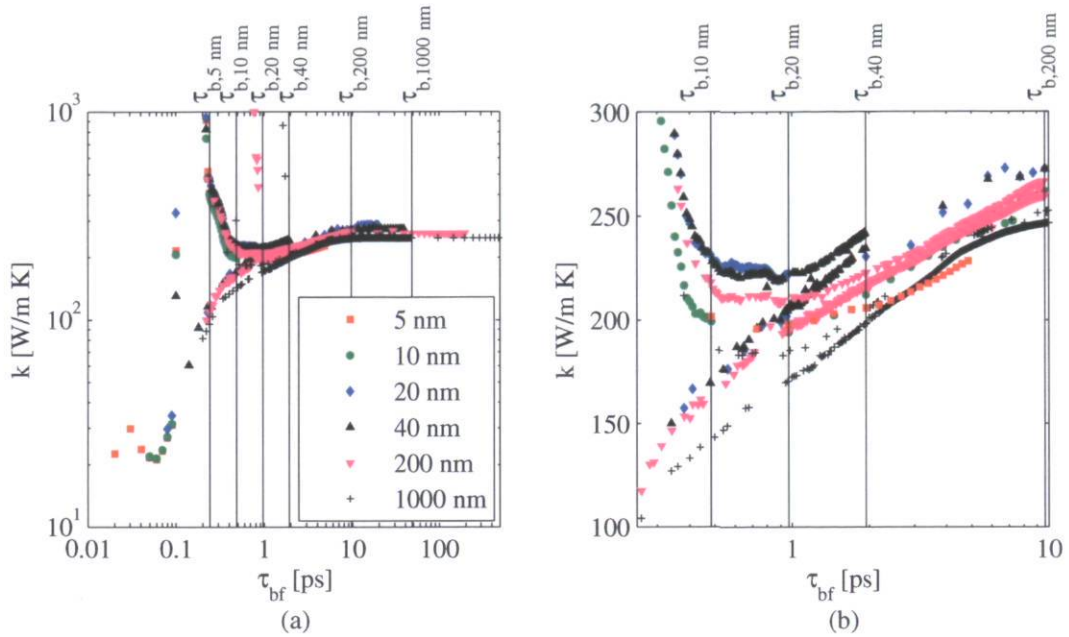

Figure 4.6: Thermal conductivity as a function of the fitting time τ_{bf} with τ_s = 2,000 ps: (a) for all lengths with only one initial condition and (b) zoom over the central part of Fig. 4.6(a)

Even though there are physical reasons that can result in a length dependence of the thermal conductivity, such as the frequency cut-off which only allows phonon modes that have wavelength smaller than the simulation box to exist, it remains difficult to observe a clear effect of length when the impact of the initial condition on the calculated thermal conductivity is so important. Efforts should be made in order to minimize the impact of the initial condition on the results by using longer simulation times and performing more simulations in order to have a better statistical precision when averaging and calculating standard errors. There is also the issue of the spurious self-correlation effects that seem negligible, since the same results could be obtained from shorter nanotubes with PBCs provided that long enough fitting times are used according to Fig. 4.6. Averages of many auto-correlation functions could also be used prior to the best-fit (or direct integration of the HCACF) in order to minimize the fluctuations of the auto-correlation function at larger times, where the statistical precision is less than that at early times.

4.7 SIMPLE EXPONENTIAL VS DOUBLE EXPONENTIAL BEST-FIT

When the fitting time is very large, such as in the zone of "converged" thermal conductivity, the time interval covering the fast initial decay of the HCACF becomes negligible as compared to the time interval covering the long, slow exponential decay. Most of the solutions of the best-fit will therefore only include a single exponential, i.e. the best-fit resulting from the minimization process is a single exponential solution. However, there are some solutions that do include a double exponential. Those solutions generally give rise to a slightly higher thermal conductivity. An example of such behavior can be seen in Fig. 4.2 for $\tau_{bf} \sim \tau_b$. There is a small number of points for one simulation (downward triangles) that are above the converged value of thermal conductivity for the same simulation. Those points have a double-exponential solution, while the others have a single exponential solution. To investigate the use of single versus double exponential best-fit, the thermal conductivity has been calculated for both cases using fitting times ~ 100 ps, which corresponds to the zone of converged thermal conductivity. The results are illustrated in Fig. 4.7 as a function of the length.

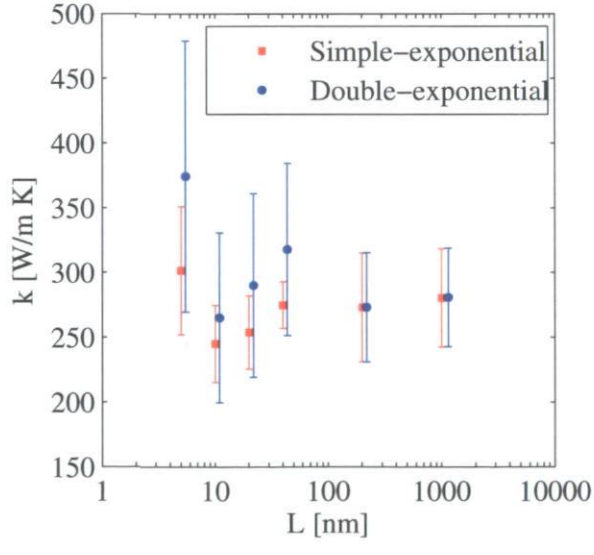

Figure 4.7: "Converged" thermal conductivity as a function of length with simple and double-exponential best-fits

A small shift in length has been introduced in Fig. 4.7 between the simple and double-exponential results at the same length for more clarity. The studied lengths are the same as in the previous sections. Each point corresponds to the mean value and standard error for the same 5 initial conditions that were previously studied. This figure shows that the oscillations between single and double exponential solutions diminish as the length increases. It also shows that higher mean values are obtained for double-exponential as compared to single-exponential best-fit. This is because when a solution includes both exponentials, the best-fit of the long exponential decay of the HCACF is not as good as when only using a single-exponential best-fit. Since it is the part that contributes the most to the thermal conductivity, it results in a significant difference in the calculated thermal conductivity. The standard error is also less important when using single-exponential best-fit for different initial conditions. Fig. 4.7 clearly shows that if the constraint of $\tau_{bf} < \tau_b$ is ignored and if the fitting time is large enough so that only the long exponential decay of the HCACF is taken into account during the fitting (converged thermal conductivity), then the calculated thermal conductivity is independent of the length of the simulated carbon nanotube.

4.8 CONCLUSIONS

Equilibrium molecular dynamics simulations of (10, 10) carbon nanotubes with periodic boundary condition in the axial direction have been performed in order to study the impact of the post-treatment of the results on the thermal conductivity. Using a method based on the impact of the initial condition on the results, a simulation time of at least 1,500 ps (1,500,000 time steps) was suggested. Much larger simulation times should however be used to obtain a sufficient statistical precision [35]. Using small simulation times can result in large standard errors, which means that even with a similar set-up, different authors could obtain different results. When using a best-fit of the auto-correlation function in conjunction with the linear response theory to estimate the thermal conductivity, the fitting time has an important impact on the calculated thermal conductivity. If small fitting times are used, there may be more than one possible solution. The two main solutions show simple and double-exponential behaviors. This

behavior could also explain some of the differences found in literature. The thermal conductivity as a function of the fitting time has been found to be independent of the length of the simulation box, i.e. the length of the carbon nanotube with PBCs. This also suggests that the length effect reported in literature could be at least in part an effect of the fitting time when using fitting times smaller than ballistic times. Furthermore, since similar results can be obtained from short nanotubes as compared to long nanotubes, the actual importance of the spurious self-correlation effect could be questioned. Using long nanotubes for the calculations means computationally expensive simulations which could be avoided by using smaller nanotubes without influencing significantly the results. This could also allow performing more simulations and getting a better statistical precision while making averages of the auto-correlation functions or of the calculated thermal conductivity. Finally, using a fitting time equal to 100 ps for all lengths, the thermal conductivity has been found to be independent of length when using PBCs.

CHAPTER 5: Influence of frequency cut-off on thermal conductivity of carbon nanotubes from EMD simulations with periodic boundary conditions

5.1 RÉSUMÉ

Ce chapitre présente les résultats d'un article court portant sur l'effet de fréquence de coupure fréquemment discuté dans la littérature lors du calcul de la conductivité thermique de nanotubes de carbone avec conditions aux limites périodiques. La densité d'états de phonons est calculées et normalisée afin d'être comparée pour des nanotubes de différentes longueurs. Tel que mentionné dans la littérature, il est possible d'observer un effet de fréquence de coupure pours les courtes fréquences. Toutefois, il est montré que cet effet de coupure a une faible influence sur le calcul de la conductivité thermique de nanotubes de carbones comparativement aux autres phénomènes numériques inhérents aux simulations de dynamique moléculaire à l'équilibre pouvant modifier les résultats, tels que ceux discutés dans les précédents chapitres.

5.2 FREQUENCY CUT-OFF PHENOMENON

The issue of predicting thermal properties of carbon nanotubes (CNTs) has been addressed in the past years by using different numerical methods, such as classical molecular dynamics [30,31], harmonic and anharmonic lattice dynamics [32,37], or more recently, the spectral energy density method [33] to name only a few. However, the discrepancies between values estimated numerically and experimentally can sometimes reach several orders of magnitude [11]. Despite advances in the development of new numerical methods, these methods are often compared to equilibrium molecular dynamics (EMD) or non-equilibrium molecular dynamics (NEMD) for validation, and these former methods continue to be widely used. On the other hand, there are still open questions regarding these methods that should be addressed. One numerical issue which

has been reported by different authors when using periodic boundary conditions (PBCs) with the EMD method is the frequency cut-off phenomenon, which states that no axial mode of wavelength larger than the simulation domain can exist [29,17]. This means that large wavelength (or small frequency) modes cannot contribute to the thermal conductivity of carbon nanotubes. It was assessed that the low frequency acoustic modes in a carbon nanotube can contribute to approximately 40% of the thermal conductivity when using the spectral energy density method [33]. However, some other works suggest that the thermal conductivity obtained by EMD simulations and the Green-Kubo formula could be similar whether small or large simulation domains were used with PBCs, see Chapter 4. Among the possible reasons are the initial condition of the system at a given temperature and the best-fitting parameters which could have a greater influence on the calculated thermal conductivity than the cut-off frequency with that method. If large enough fitting times were used for the best-fit of the auto-correlation function in Chapter 4, the thermal conductivity was nearly independent of the nanotube length. In this work, we first address the influence of the initial condition of the system on the frequency cut-off phenomenon by calculating the axial phonon density of states. We then compare the results for different nanotube lengths and determine if the initial condition could influence the frequency cut-off phenomenon in such a way that the calculated thermal conductivity of carbon nanotubes would be independent of the nanotube length when using periodic boundary conditions.

In order to estimate the phonon density of states, it is first required to calculate the velocity auto-correlation function from MD simulation data. Such simulations have been performed for (10, 10) CNTs of length varying from 5 nm to 1000 nm (enough to reach a fully diffusive regime) with the REBO potential [23] and the thermal conductivity has been calculated using the EMD method with the Green Kubo formalism [30]. Simulations were divided in three steps: (1) a 100 ps run in the microcanonical ensemble (constant number of atoms, volume, and energy) to allow the system to reach equilibrium, (2) a 400 ps run in the canonical ensemble (constant number of atoms, volume, and temperature) to bring the system to the desired temperature of 300 K, and (3) a 2 ns run in the microcanonical ensemble during which the instantaneous axial heat

flux and atom velocities are recorded in output files for the calculation of the thermal conductivity and axial phonon density of states. Due to the large amount of data generated for long nanotubes, the axial velocity for each atom has been recorded only for the first 6.5 ps. The time step for all simulations is 1 fs. More details on the simulation procedure can be found in Chapters 3 and 4. Once the axial velocity of each atom is known, the axial phonon density of states (DOS_z) for a system of N atoms is given by [8]

$$DOS_z(\omega) = \frac{1}{N}\sum_{j=1}^{N} FFT\left[\left\langle v_z^j(t)\cdot v_z^j(0)\right\rangle\right] \tag{5.1}$$

where v_z^j and $\left\langle v_z^j(t)\cdot v_z^j(0)\right\rangle$ are the axial velocity and velocity auto-correlation function of the j^{th} atom of the system, and FFT is the Fast Fourier Transform of the quantity between brackets. The axial DOS given in Eq. (5.1) is in arbitrary units. The only normalization factor that has been considered in the present work is the total number of atoms of the system, in order to allow comparison between densities of states of nanotubes of different lengths (i.e. different size of the simulation domain with PBCs), since all simulations are performed at the same temperature (300 K). Physically, the density of states represents the number of vibrational states per unit frequency. In other words, the stronger the peak at a given frequency, the more populated that vibrational mode in the carbon nanotube.

As an example, the longitudinal phonon density of states (arbitrary units) for a 200 nm long (10, 10) carbon nanotube is shown in Fig. 5.1. The number of time steps used to calculate all density of states is such that the spectral resolution is about 0.1 THz. Fig. 5.1 shows the average (middle curve), minimum (lower curve), and maximum (upper curve) values of the DOS calculated from the results of 5 simulations with different initial conditions (different orientation of the velocity vectors of the atoms) at the same temperature. The resulting DOS is very similar to other DOS found in literature and shows a strong peak near 52 THz, which is characteristic of the phonon spectrum of a graphene sheet [38]. There are also no strong peaks at low frequency due to boundary scattering, since PBCs have been used in all simulations [11].

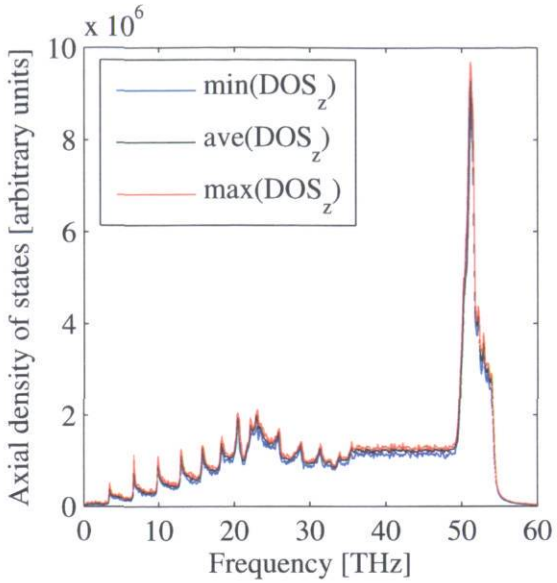

Figure 5.1: Axial phonon density of states for a 200 nm long carbon nanotube with PBCs

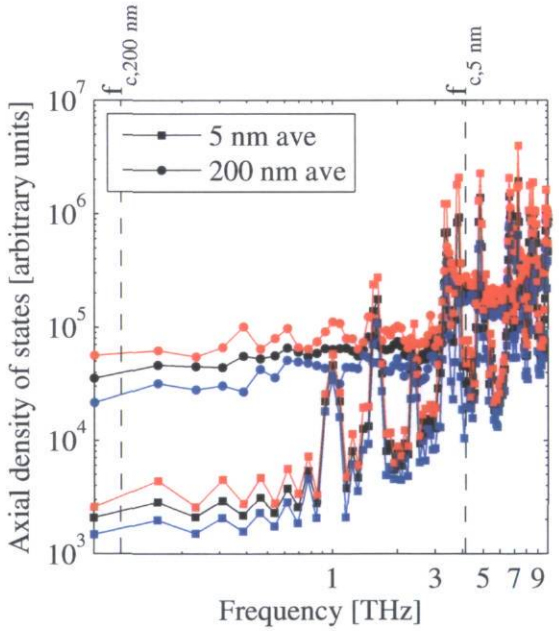

Figure 5.2: Comparison of the axial phonon density of states for 5 and 200 nm long carbon nanotubes at low frequencies (min: blue, ave: black, and max: red)

The impact of the initial condition on the DOS (i.e. the distance between the min and max curves), although hardly visible in Fig. 5.1, varies between 100% of the average DOS (at low frequencies) and 20% (at high frequencies). However, even though there is a significant variation in amplitude, the peaks in the DOS appear at the same frequencies. Fig. 5.2 shows the longitudinal density of states for 5 and 200 nm long carbon nanotubes in the low frequency range. In this figure, the average (middle curves), minimum (lower curves), and maximum (upper curves) values of the DOS are also shown for both lengths as explained previously. As can be seen in Fig. 5.2, the variations of the DOS caused by different initial conditions does not result in any cross-over between the DOS calculated from nanotubes of different lengths at low frequencies. A conservative estimate of the frequency cut-off can be obtained by taking the ratio of the speed of sound of the longitudinal acoustic mode (CLA ~ 20.35 km/s [13]) to the length of the nanotube. This corresponds to the inverse of the time required for a phonon to ballistically pass through the nanotube. For nanotube lengths of 5 and 200 nm, the frequency cut-off thus corresponds to approximately 4 and 0.1 THz. These frequencies are indicated in Fig. 5.2 by vertical dotted lines. As can be observed in Fig. 5.2, there is a notable difference in amplitude between both DOS at frequencies below the frequency cut-off of the 5 nm long nanotube (cut-off effect). This difference in amplitude is sufficiently large for the frequency cut-off not to be influenced by the variation of the initial condition. In other words, the initial condition does not affect the density of states enough to prevent the frequency cut-off phenomenon. This might suggest that the frequency cut-off in carbon nanotubes could influence the calculated thermal conductivity of carbon nanotubes when using EMD simulations, since long wavelength modes are not present in small nanotubes and therefore cannot contribute to its thermal conductivity. However, the results presented in Fig. 5.3, adapted from Chapter 4, do not support that statement. As it is often done, a double-exponential best-fit of the heat current auto-correlation function was integrated in the following equation to estimate the thermal conductivity according to the Green Kubo formula:

$$k = \frac{1}{k_B T^2 LA} \int_0^\infty \langle j_z(0) j_z(t) \rangle \, dt \tag{5.2}$$

where k_B is the Boltzmann constant, T is the temperature of the system (taken as the average of the mean temperature of the system during the simulation), L and A are the length and cross-sectional area of the nanotube, and j_z is the axial component of the heat current. Note that there are different conventions for the cross-sectional area of a nanotube [11], but the one used in all simulations is a ring with a thickness equal to 3.4 Å. In Eq.(5.2), $\langle j_z(0) j_z(t) \rangle$ is called the heat current auto-correlation function (HCACF). In all simulations, a method based on fast Fourier transform is used to calculate this function. The thermal conductivity obtained from Eq. (5.2) is plotted in Fig. 5.3 as a function of the fitting time τ_{bf} of the heat current auto-correlation function for 5 and 200 nm long carbon nanotubes. Lower and upper error bars in Fig. 5.3 correspond to the minimum and maximum thermal conductivity among 5 simulations with different initial conditions at the same temperature using the previously described procedure. Other nanotube lengths have been tested and the same trends have been observed, see Chapter 4. Results in Fig. 5.3 clearly show that the initial condition of the system, even at the same temperature, will influence the calculated thermal conductivity and there will be a cross-over of the results for short and long nanotubes. The influence of the initial condition on the calculated thermal conductivity (i.e. sum of the upper and lower error bars in Fig. 5.3) varies from 20 to 60% of the average thermal conductivity. This variation is of the same order of magnitude as that of the DOS calculated previously. From the results presented in Fig. 5.3, one could conclude that even if the frequency cut-off is not influenced by the initial condition (i.e. the frequency cut-off phenomenon will be present for small length when using different initial conditions), it appears negligible compared to the influence of the initial condition (or of the fitting time) on the calculated thermal conductivity. It also means that if large enough fitting times are used, the calculated thermal conductivity when performing EMD simulations with PBCs and when using the Green-Kubo method is only weakly influenced by length.

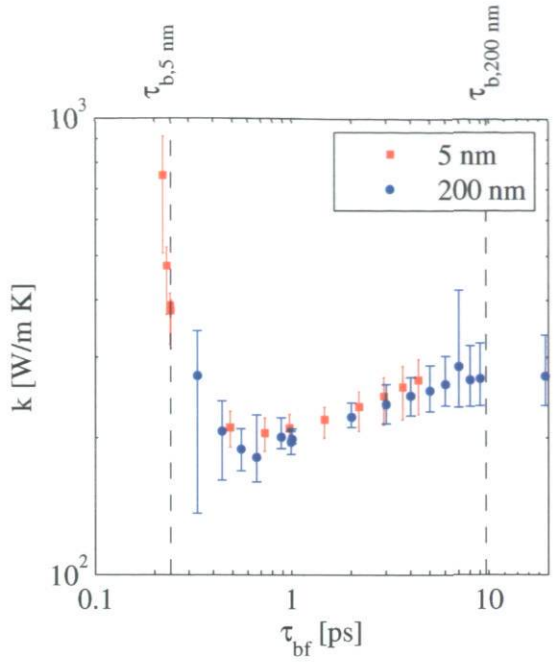

Figure 5.3: Thermal conductivity as a function of the fitting time τ_{bf} for 5 and 200 nm long carbon nanotubes

5.3 CONCLUSIONS

In summary, the axial phonon density of states has been calculated from EMD simulations with PBCs and the Green-Kubo formalism for carbon nanotubes of different lengths in order to investigate the importance of the initial condition on the frequency cut-off phenomenon. It has been shown that the frequency cut-off phenomenon is present for short nanotubes regardless of the initial condition at a given temperature and therefore that low-frequency modes could not contribute to the thermal conductivity. However, it has been demonstrated that when calculating the thermal conductivity, the impact of other simulation and modeling parameters (such as the initial condition or the fitting time) will influence the results in such a way that the cut-off phenomenon appears negligible.

CONCLUSIONS

In the first part of the present work, modeling and simulation parameters that influence the calculated thermal conductivity of a carbon nanotube when performing EMD simulations have been identified. After a literature review, it has been determined that the most important parameters were the nanotube length (which is related to the frequency cut-off phenomenon), the simulation time (number of time steps), the inter-atomic potential used to model the forces between the atoms of the nanotube, and the fitting time used for the best-fit of the auto-correlation function (related to the spurious self-correlation effect). In Chapter 3, a preliminary study on the effect of those parameters on the calculated thermal conductivity has been done for a 5 nm long (10, 10) carbon nanotube. It was demonstrated that it is important to use a large enough simulation time in order to minimize the impact of the initial condition of the system (different initial orientation of the velocity vectors of the atom, but at the same temperature). For this reason, a simulation time of at least 2,000 ps was suggested. For such small nanotubes, it was shown that using a fitting time smaller than the ballistic time could lead to an underestimation of the thermal conductivity, since only the fast initial decay of the heat current auto-correlation function was taken into account. In Chapter 4, carbon nanotubes of different lengths were studied. It was found that if large enough fitting times were used, similar thermal conductivities could be obtained regardless of the length. That was in contradiction with some of the results found in literature which stated that there was a length effect when calculating the thermal conductivity of carbon nanotubes, mainly due to the frequency cut-off phenomenon. In order to determine if the importance of this phenomenon, the density of states has been calculated and the results were presented in Chapter 5. It was found that the frequency cut-off phenomenon does exist, but it is negligible as compared to the effect of the other simulation parameters, such as the initial condition, when performing EMD simulations with the Green-Kubo method.

In light of the results obtained in the present work, it is possible to explain, at least in part, some of the discrepancies found in literature, which was one of the objectives of this work. The impact of the simulation time is crucial to minimize the impact of the initial

condition on the calculated thermal conductivity. Many authors used a simulation time smaller than 2,000 ps, which could lead to large variations of the thermal conductivity calculated by different authors. Furthermore, some authors have used different fitting times for different lengths and observed a length effect, but it is possible that this would rather be, at least in part, a fitting time effect (corresponding to the lower branch in Fig. 4.6). Others have used the same fitting time for different lengths, but the variation of the thermal conductivity due to the initial condition is so large that no clear length effect could be observed. Finally, Fig. 4.6 itself shows that for the same simulation, there is non-uniqueness of the solution when using a best-fit of the auto-correlation function. In some cases, the calculated thermal conductivity could differ by many orders of magnitudes. That is another possible explanation for the discrepancies in literature. It is important to mention that these explanations are valid only for EMD simulations with the Green-Kubo method. Simulations with different methods would need to be performed in order to determine if the simulation parameters have the same importance in all cases.

It would be interesting to study nanotubes in a more concrete application, such as a thermal gradient driven nanomotor. This device is made of two concentric carbon nanotubes, where a motion of the outer nanotube is induced by applying a thermal gradient on the inner nanotube. The type of motion induced is determined by the chiralities of both carbon nanotubes. It could thus be interesting to study the effect of applying mechanical stress on the inner tube on the motion of the nanomotor. The expertise developed in the present work could be useful in determining the thermal conductivity of the inner nanotube under mechanical stress. It could also be interesting to determine if it would be possible to tune the thermal conductivity of the inner tube in order to control the motion of the nanometer (translational, rotational, or a combination of both).

REFERENCES

1 Iijima S., Helical Microtubules of Graphitic Carbon, Nature, Vol. 354 (1991), pp. 56-58.

2 Hone J., Whitney M., Piskotti C., and Zettl A., Thermal Conductivity of Single-Walled Carbon Nanotubes, Physical Review B, Vol. 59 (2008), pp. R2514-R2516.

3 Kim P., Shi L., Majumdar A., and McEuen P.L., Thermal Transport Measurements of Individual Multiwalled Nanotubes, Physical Review Letters, Vol. 87 (2001), pp. 215502.

4 Fujii M., Zhang X., Xie H., Ago H., Takahashi K., and Ikuta T., Measuring the Thermal Conductivity of a Single Carbon Nanotube, Physical Review Letters, Vol. 95 (2005), pp. 065502.

5 Yu C.H., Shi L., Yao Z., Li D.Y., and Majumdar A., Thermal Conductance and Thermopower of an Individual Single-Wall Carbon Nanotube, Nano Letters, Vol. 95 (2005), pp. 1842-1846.

6 Choi T.-Y., Poulikakos D., Tharian J., and Sennhauser U., Measurement of the Thermal Conductivity of Individual Carbon Nanotubes by the Four-Point Three-ω Method, Nano Letters, Vol. 6 (2006), pp. 1589-1593.

7 Pop E., Mann D., Wang Q., Goodson K. and Dai H., Thermal Conductance of an Individual Single-Wall Carbon Nanotube Above Room Temperature, Nano Letters, Vol. 6 (2006), pp. 96-100.

8 Ren C., Zhang W., Xu Z., Zhu Z., and Huai P., Thermal Conductivity of Single-Walled Carbon Nanotubes Under Axial Stress, Journal of Physical Chemistry, Vol. 114 (2010), pp. 5786-5791.

9 Li X., Liu J., and Yang R., Tuning Thermal Conductivity with Mechanical Strain, Proceedings of the 14th International Heat Transfer Conference, Washington, DC, USA, August 8 – 13 (2010), pp. 23334.

10 Guo Z.-X. and Gong X.-G., Molecular Dynamics Studies on the Thermal Conductivity of Single-Walled Carbon Nanotubes, Frontiers of Physics in China, Vol. 4 (2009), pp. 389-392.

11 Lukes J. R. and Zhong H., Thermal Conductivity of Individual Single-Wall Carbon Nanotubes, Journal of Heat Transfer, Vol. 129 (2007), pp. 705-716.

12 Reilly R. M., Carbon Nanotubes: Potential Benefits and Risks of Nanotechnology in Nuclear Medicine, The Journal of Nuclear Medicine, Vol. 48 (2007), pp. 1039-1042.

13 Dresselhaus M. S. and Eklund P. C., Phonons in Carbon Nanotubes, Advances in Physics, Vol. 49 (2008), pp. 705-814.

14 Plimpton S., Fast Parallel Algorithms for Short-Range Molecular Dynamics, Journal of Computational Physics, Vol. 117 (1995), pp. 1-19.

15 http://lammps.sandia.gov, July 19, 2011.

16 Chen G., Nanoscale Energy Transport and Conversion – A Parallel Treatment of Electrons, Molecules, Phonons, and Photons, Oxford University Press, New-York (2005), pp. 130-134; 452-504.

17 Volz S. G. and Chen G., Molecular-Dynamics Simulation of Thermal conductivity of Silicon Crystals, Physical Review B, Vol. 61 (2000), pp. 2651-2656.

18 Goldstein H., Classical Mechanics, Addison-Wesley Publishing Company (1980), pp. 188-192.

19 Tersoff J., New Empirical Approach for the Structure and Energy of Covalent Systems, Physical Review B, Vol. 37 (1988), pp. 6991-7000.

20 Tersoff J., Modeling Solid-State Chemistry: Interatomic Potentials for Multicomponent Systems, Physical Review B, Vol. 39 (1989), pp. 5566-5568.

21 Brenner D. W., Empirical Potential for Hydrocarbons for Use in Simulating the Chemical Vapor Deposition of Diamond Films, Physical Review B, Vol. 42 (1990), pp. 9458-9471.

22 Brenner D. W., Erratum: Empirical Potential for Hydrocarbons for Use in Simulating the Chemical Vapor Deposition of Diamond Films, Physical Review B, Vol. 46 (1992), pp. 1948.

23 Brenner D. W., Shenderova O. A., Harrison J. A., Stuart S. J., Ni B., and Sinnott S. B., A Second-Generation Reactive Empirical Bond Order (REBO) Potential

Energy Expression for Hydrocarbons, Journal of Physics: Condensed Matter, Vol. 14 (2002), pp. 783-802.

24 Stuart S. J., Tutein A. B., and Harrison J. A., A Reactive Potential for Hydrocarbons with Intermolecular Interactions, Journal of Chemical Physics, Vol. 112 (2000), pp. 6472-6486.

25 Lindsay L. and Broido D. A., Optimized Tersoff and Brenner Empirical Potential Parameters for Lattice Dynamics and Phonon Thermal Transport in Carbon Nanotubes and Graphene, Physical Review B, Vol. 81 (2010), pp. 205441.

26 Allen M. P. and Tildesley D. J., Computer Simulation of Liquids, Oxford University Press, New-York (1989), pp. 185-191.

27 Osman M. A. and Srivastava D., Temperature Dependence of the Thermal Conductivity of Single-Wall Carbon Nanotubes, Nanotechnology, Vol. 12 (2001), pp. 21-24.

28 Maruyama S., A Molecular Dynamics Simulation of Heat Conduction of a Finite Length Single-Walled Carbon Nanotube, Microscale Thermophysical Engineering, Vol. 7 (2003), pp. 41-50.

29 Grujicic M., Cao G., and Roy W. N., Computational Analysis of the Lattice Contribution to Thermal Conductivity of Single-Walled Carbon Nanotubes. Journal of Material Science, Vol. 40 (2005), pp. 1943-1952.

30 Frenkel D. and Smit B., Understanding Molecular Simulation: from Algorithms to Applications, second ed., Academic Press, San Diego (2002).

31 Hoover W. G. and Ashurst W. T., Theoretical Chemistry: Advances and Perspectives, Academic Press, New-York (1975).

32 Turney J. E., Landry E. S., McGaughey A. J. H., and Amon C. H., Predicting Phonon Properties and Thermal Conductivity from Anharmonic Lattice Dynamics Calculations and Molecular Dynamics Simulations, Physical Review B: Condensed Matter and Materials Physics, Vol. 79 (2009), pp. 064301.

33 Thomas J. A., Turney J. E., Iutzi R. M., Amon C. H., and McGaughey A. J. H., Predicting Phonon Dispersion Relations and Lifetimes from the Spectral Energy Density, Physical Review B: Condensed Matter and Materials Physics, Vol. 81 (2010), pp. 081411.

34 Che J., Cagin T., and Goddard III W. A., Thermal Conductivity of Carbon Nanotubes, Nanotechnology, Vol. 11 (2000), pp. 65-69.

35 Donadio D. and Galli G., Thermal Conductivity of Isolated and Interacting Carbon Nanotubes: Comparing Results from Molecular Dynamics and the Boltzmann Transport Equation, Physical Review Letters, Vol. 99 (2007), pp. 255502.

36 Lagarias J. C., Reeds J. A., Wright M. H., and Wright P. E., Convergence Properties of the Nelder-Mead Simplex Method in Low Dimensions, SIAM Journal of Optimization, Vol. 9 (1998), pp.112-147.

37 Debernardi A., Baroni S., and Molinari E., Anharmonic Phonon Lifetimes in Semiconductors from Density Functional Perturbation Theory, Physical Review Letters, Vol. 75 (1995), pp. 1819-1822.

38 Sokhan V. P., Nicholson D., and Quirke N., Phonon Spectra in Model Carbon Nanotubes, Journal of Chemical Physics, Vol. 113 (2000), pp. 2007-2015.

APPENDIX 1: SIMULATION.TXT SAMPLE FILE

```
# Setting up simulation
units           metal
boundary        f       f       p
neigh_modify    delay       0       every       1       check       no
read_data       atomData.txt
pair_style      airebo  5.0  0  0
pair_coeff      *  *  CH.airebo  C
timestep        0.001

# Defining groups of atoms
group       inner          type  1
group       bounded   id <=    160000
group       notFixed       id    <=     160000

# Computing potential and kinetic energy per atom, stress per atom, and heat flux
compute     pePerAtomB          bounded          pe/atom
compute     kePerAtomB          bounded          ke/atom
compute     stressPerAtomB      bounded          stress/atom    virial
compute heatFluxB bounded heat/flux kePerAtomB pePerAtomB stressPerAtomB

# Print thermodynamic properties in log file (output file)
compute     myTemp      bounded   temp
thermo      1
thermo_style  custom    step   c_myTemp   c_heatFluxB[3] c_heatFluxB[6]
thermo_modify       format  2  %25.15e
thermo_modify       format  3  %25.15e
thermo_modify       format  4  %25.15e
```

 # NVE integration scheme

```
fix     fix_nve   notFixed   nve
run             100000
```

 # NVT integration scheme

```
unfix   fix_nve
fix     fix_nvt   notFixed   nvt   temp   300   300   0.001
run             400000
```

 # NVE integration scheme

```
unfix   fix_nvt
fix     fix_nve   notFixed   nve
reset_timestep 0
restart 500000 *.restart
log     simuLOG.0.txt
run       500000
log     simuLOG.500000.txt
run       500000
log     simuLOG.1000000.txt
run       500000
log     simuLOG.1500000.txt
run       500000
```